NASA/TM—2007-214921

Assessment of Creep Capability of HSR–EPM Turbine Airfoil Alloys

Rebecca A. MacKay
Glenn Research Center, Cleveland, Ohio

Anita Garg
University of Toledo, Toledo, Ohio

Frank J. Ritzert
Glenn Research Center, Cleveland, Ohio

Ivan E. Locci
University of Toledo, Toledo, Ohio

December 2007

NASA STI Program . . . in Profile

Since its founding, NASA has been dedicated to the advancement of aeronautics and space science. The NASA Scientific and Technical Information (STI) program plays a key part in helping NASA maintain this important role.

The NASA STI Program operates under the auspices of the Agency Chief Information Officer. It collects, organizes, provides for archiving, and disseminates NASA's STI. The NASA STI program provides access to the NASA Aeronautics and Space Database and its public interface, the NASA Technical Reports Server, thus providing one of the largest collections of aeronautical and space science STI in the world. Results are published in both non-NASA channels and by NASA in the NASA STI Report Series, which includes the following report types:

- TECHNICAL PUBLICATION. Reports of completed research or a major significant phase of research that present the results of NASA programs and include extensive data or theoretical analysis. Includes compilations of significant scientific and technical data and information deemed to be of continuing reference value. NASA counterpart of peer-reviewed formal professional papers but has less stringent limitations on manuscript length and extent of graphic presentations.

- TECHNICAL MEMORANDUM. Scientific and technical findings that are preliminary or of specialized interest, e.g., quick release reports, working papers, and bibliographies that contain minimal annotation. Does not contain extensive analysis.

- CONTRACTOR REPORT. Scientific and technical findings by NASA-sponsored contractors and grantees.

- CONFERENCE PUBLICATION. Collected papers from scientific and technical conferences, symposia, seminars, or other meetings sponsored or cosponsored by NASA.

- SPECIAL PUBLICATION. Scientific, technical, or historical information from NASA programs, projects, and missions, often concerned with subjects having substantial public interest.

- TECHNICAL TRANSLATION. English-language translations of foreign scientific and technical material pertinent to NASA's mission.

Specialized services also include creating custom thesauri, building customized databases, organizing and publishing research results.

For more information about the NASA STI program, see the following:

- Access the NASA STI program home page at *http://www.sti.nasa.gov*

- E-mail your question via the Internet to *help@sti.nasa.gov*

- Fax your question to the NASA STI Help Desk at 301–621–0134

- Telephone the NASA STI Help Desk at 301–621–0390

- Write to:
  NASA Center for AeroSpace Information (CASI)
  7115 Standard Drive
  Hanover, MD 21076–1320

NASA/TM—2007-214921

Assessment of Creep Capability of HSR–EPM Turbine Airfoil Alloys

Rebecca A. MacKay
Glenn Research Center, Cleveland, Ohio

Anita Garg
University of Toledo, Toledo, Ohio

Frank J. Ritzert
Glenn Research Center, Cleveland, Ohio

Ivan E. Locci
University of Toledo, Toledo, Ohio

National Aeronautics and
Space Administration

Glenn Research Center
Cleveland, Ohio 44135

December 2007

Acknowledgments

The authors would like to express their appreciation to Dr. Ajay K. Misra and Mr. Robert D. Draper of the Ultra Efficient Engine Technology (UEET) Program Office for supporting this work under RTOP 714–04–20. Rebecca MacKay would also like to acknowledge Dr. Richard Grylls of GE Aircraft Engines, Dr. Alan Cetel of Pratt & Whitney, and Dr. James L. Smialek and Dr. Michael V. Nathal of NASA Glenn Research Center for many useful discussions. This research was originally published internally as UEET001 in February 2001.

Trade names and trademarks are used in this report for identification only. Their usage does not constitute an official endorsement, either expressed or implied, by the National Aeronautics and Space Administration.

This work was sponsored by the Fundamental Aeronautics Program at the NASA Glenn Research Center.

Level of Review: This material has been technically reviewed by technical management.

Available from

NASA Center for Aerospace Information
7115 Standard Drive
Hanover, MD 21076–1320

National Technical Information Service
5285 Port Royal Road
Springfield, VA 22161

Available electronically at http://gltrs.grc.nasa.gov

Assessment of Creep Capability of HSR–EPM Turbine Airfoil Alloys

Rebecca A. MacKay
National Aeronautics and Space Administration
Glenn Research Center
Cleveland, Ohio 44135

Anita Garg
University of Toledo
Toledo, Ohio 43606

Frank J. Ritzert
National Aeronautics and Space Administration
Glenn Research Center
Cleveland, Ohio 44135

Ivan E. Locci
University of Toledo
Toledo, Ohio 43606

Introduction

The High Speed Civil Transport (HSCT) mission of the High Speed Research-Enabling Propulsion Materials (HSR-EPM) Program represented a unique challenge for turbine airfoil materials [1]. The highest operating temperatures in the HSCT mission occur during climb and *supersonic* cruise, which amounts to hours at the highest operating temperatures during each flight. Thus, the accumulated hot time of an HSCT engine before overhaul is many thousands of hours [1]. In contrast, in current *subsonic* engines, the maximum operating temperatures occur during takeoff and thrust reverse after landing, which amounts to only 2 to 5 minutes at the highest operating temperatures during each flight. Accumulated hot time before overhaul is about 300 hours for a typical subsonic engine [1].

Current turbine airfoils are composed of a material system consisting of a single crystal superalloy base that provides the basic mechanical performance of the airfoil, a thermal barrier coating (TBC) that reduces the temperature of the base superalloy, and a bondcoat between the superalloy and the TBC. The bondcoat improves resistance to oxidation and corrosion and also improves the spallation resistance of the TBC. A similar material system was to be optimized under the HSR-EPM Program and combined with advances in airfoil cooling technology to meet the structural and long-term durability requirements of the HSCT mission.

The goal of airfoil alloy development under the HSR-EPM Program was to develop an alloy with a $+75^{o}$F increase in creep rupture capability over the average René N5/PWA 1484 baseline. Other goals are specified and discussed in the annual [2-6] and final [1] reports, including the goal of microstructural stability sufficient to avoid degradation of long-time properties.

Airfoil alloy development under the HSR-EPM Program pursued a path that led to evolutionary mechanical behavior improvements. The EPM airfoil alloys contain increased amounts of rhenium in the pursuit of high strength at higher temperatures. Since alloys with improved strength are obtained when the limits of microstructural stability are approached or exceeded slightly, some of the EPM airfoil alloys exhibited microstructural instabilities. These observed instabilities include TCP (topologically close packed) phases and a reaction that has been termed SRZ (secondary reaction zone) [7]. Excessive quantities of either TCP or SRZ can severely decrease the mechanical properties [1,5].

After several iterative alloying campaigns throughout the duration of the HSR-EPM Program, EPM102 was identified as an alloy that exhibited the best balance of creep strength and stability with respect to TCP and SRZ formation. EPM102 was thus selected for further compositional optimization. In the final airfoil alloying campaign in the program, the EPM102 composition was varied with respect to aluminum (Al) and cobalt (Co). Increases in Al content had been shown during the program [1] to increase creep-rupture strength and to decrease microstructural stability. Increases in Co content had been shown [1] to reduce the SRZ that formed under the bondcoat while reducing uncoated oxidation resistance. Four compositions were chosen to define the optimum combination of these two elements in the baseline EPM102 alloy; these were designated as EPM102A, EPM102B, EPM102C, and EPM102D. EPM102A was designed to be compositionally identical to the baseline EPM102 alloy.

Howmet-Dover produced 1500-lb. master heats of each of the four compositions. Pratt & Whitney conducted chemical analyses on the master heats, which showed that the analyzed compositions were close to the aim levels, with the exception of the Al content in EPM102B, EPM102C, and EPM102D. In an attempt to reach the desired Al levels in these alloys, additions of Al were made to the master heats during the subsequent casting of single crystal slabs at PCC-Minerva. Two different Al additions were intentionally introduced during the casting of EPM102B, at the request of NASA Glenn Research Center (NASA GRC), to evaluate the effect of high Al contents. Furthermore, two slab molds of EPM102C were also cast with no Al additions to examine another Al variation. Table I [1,6] lists the original aim composition for each alloy, along with the analyzed composition of the master heat and the analyzed composition of one single crystal slab from each mold. Pratt & Whitney conducted all of these chemical analyses [1,6]. A "+" designation in Table I identifies the slabs to which Al was added during casting.

During the last few months of the HSR-EPM Program, characterization of EPM102A, EPM102C, EPM102C+, and EPM102D+ was conducted. Most of this characterization was performed by Pratt & Whitney and GE Aircraft Engines on bare, or uncoated, alloys without a PtAl bondcoat. This work included uncoated creep rupture testing at 1800 and 2000^{o}F, coated creep rupture testing at 2100^{o}F, uncoated oxidation testing at 2200^{o}F, coated and uncoated high-cycle fatigue testing at 1200 and 1800^{o}F, uncoated low-cycle fatigue testing at 1200 and 1400^{o}F, and microstructural stability examinations. The reader is referred to Reference 1 for a full description of these results. EPM102B+ and EPM102B++ alloys were not tested under the HSR-EPM Program but were delivered to NASA GRC for subsequent evaluation under a future program.

The purpose of the present paper is to describe the experimental work that was performed at NASA GRC after the HSR-EPM Program ended. Emphasis will be placed on the *coated* creep properties, since little of that was obtained during the HSR-EPM Program. An understanding of the behavior of the single crystal material with the PtAl bondcoat is crucial, because the EPM alloys in a prior round (Round 4) exhibited significant debits in creep properties in coated specimens. This decrease in the mechanical properties of the Round 4 alloys after coating was attributed to the formation of SRZ [1,5] under the bondcoat. As a result of this observation, a large SRZ-reduction effort was undertaken at GE Aircraft Engines and NASA GRC during the HSR-EPM Program in order to understand and reduce SRZ formation through various surface treatments and heat treatments.

Thus, the present paper will compare the 1800^{o}F creep lives of coated single crystals to the 1800^{o}F lives that were generated on uncoated alloys during the HSR-EPM Program. Many of the coated single crystals were also given various treatments to reduce the SRZ formation during subsequent creep exposures. The efficacy of these various SRZ reduction techniques will also be discussed based on the observed microstructures and resultant creep properties. Some interrupted creep testing at 1800^{o}F was performed to examine the development and progression of phase instabilities during creep deformation prior to failure. Additional selected specimens were given an extended 2000^{o}F exposure in order to form significant quantities of SRZ under the PtAl coating prior to creep rupture testing; these experiments were designed to determine the impact of SRZ when present in large quantities at the start of the creep rupture test. The work described in this report was performed at NASA GRC, except where noted otherwise. Particular attention will be given to reporting the site at which the various tasks were performed, as it will become clear that this is an important contributor to the explanation of the observed results.

Materials and Procedures

Two single crystal molds of EPM102A, EPM102C, EPM102C+, and EPM102D+ were produced at PCC-Minerva under the HSR-EPM Program; each mold consisted of five 0.25-in. thick slabs and five 0.625-in. thick slabs. The Al additions that were introduced to produce the "+" compositions were done separately to each mold. Two different Al additions were intentionally introduced during the single crystal casting of EPM102B which resulted in one mold each of the EPM102B+ and EPM102B++ alloys. The Y additions were also accomplished during casting of the single crystal molds. Slab castings were solution treated at 2400°F for 6 hours at PCC-Minerva. The slabs were then chemically etched and electrolytically etched to reveal grain defects; Laue X-ray diffraction was also performed on each slab at PCC-Minerva to determine primary crystallographic orientations. Pratt & Whitney conducted chemical analyses of the slabs and master melt [1] using inductively coupled plasma emission spectroscopy, Table I. Creep specimens were machined from the 0.25-in. thick slabs; the threaded creep specimens had a 0.125-inch diameter gage, a 0.750-inch nominal gage length, and an overall length of 2.25 inches.

Pratt & Whitney and GE Aircraft Engines were each responsible for processing coated and uncoated creep specimens for delivery to NASA GRC for subsequent creep testing. Pratt & Whitney provided fifty PtAl-coated specimens as well as eight uncoated specimens to NASA GRC. Most of the creep specimens provided by Pratt & Whitney had been given a stress relief heat treatment at 2050°F for 4 hours after machining. Next, the specimens that were to be coated had the PtAl bondcoat applied in a proprietary process by Howmet-Thermatech. These coated specimens were subsequently delivered to NASA GRC for the post-coating heat treatments to be performed prior to testing. The post-coating treatments consisted of an age at 1975°F for 0.25 hours followed by an air cool and a subsequent age for 12 hours at 1600°F. The coated specimens provided by Pratt & Whitney were used primarily for the interrupted creep testing experiments. The eight uncoated, machined specimens were fully heat treated by Pratt & Whitney; these specimens were given a stress relief heat treatment at 2050°F for four hours, a simulated PtAl coating cycle of 1975°F for 16 hours, followed by a gas quench and a 1600°F age for 12 hours. The goal was to produce similar initial γ-γ′ microstructures in the coated and uncoated specimens prior to testing. Specimens (coated and uncoated) were also provided for examining the effects of extended aging for 400hr at 2000°F prior to creep-rupture testing; the extended ages were performed at NASA GRC.

GE Aircraft Engines supplied NASA GRC with thirty-eight machined creep specimens that had been given various SRZ-reduction treatments prior to PtAl-coating. These included either 1) a stress relief heat treatment of 2050°F for 4 hour, 2) a 2-hour carburization treatment at 2000°F, or 3) a stress relief heat treatment of 2050°F for 4 hours and the 2000°F/2 hr carburization treatment. The carburization process was performed at a GE Aircraft Engine vendor. The PtAl-coating was then applied by Howmet-Thermatech. All thirty-eight specimens were given the post coating treatment by GE Aircraft Engines, which consisted of re-aging the samples at 1975°F for 0.25 hours, gas quenching, and a subsequently aging for 12 hours at 1600°F. The coated specimens provided by GE Aircraft Engines would be subsequently tested at NASA GRC for comparison to the uncoated specimens tested during the HSR-EPM program by a Pratt & Whitney vendor. Prior to creep testing, the initial γ′ size and morphology was examined in selected specimens at NASA GRC.

Creep testing was performed in air at 1800°F and an applied stress level of 45ksi at NASA GRC according to ASTM-E 139-96 [8]. V-notches were ground into the specimen shoulders for creep extensometer attachment. Temperatures along the specimen gage length were maintained to ± 2°F. The loads that were applied to the coated specimens were based on the pre-coated diameters provided by GE Aircraft Engines and Pratt & Whitney for the specimens they respectively provided. After testing, the final specimen dimensions were measured, and the specimens were sectioned for microstructural examination. Numerous microstructural features were examined after creep rupture including prevalence of SRZ and TCP, location of secondary cracking, γ-γ′ morphologies, and the coating-substrate diffusion zone.

SRZ formation was examined on unetched specimens using back-scattered scanning electron microscopy (SEM). The SRZ thickness and the percentage of the specimen periphery that was covered by SRZ beneath the PtAl coating were measured. The average percent coverage of the SRZ, as well as the mean and maximum SRZ thicknesses, were obtained from longitudinal and transverse sections of the failed creep rupture specimens. TCP formation within the failed rupture specimens was revealed using an etchant of 33% $C_2H_4O_2$, 33% HCl, 33% H_2O, and 1% HF and was examined by SEM at a magnification of 1000X. The stain etch and optical microscopy technique that was employed in the HSR-EPM Program [1] was also used at NASA GRC to reveal TCP and produced similar results to

the above-mentioned procedure. After etching, the TCP level was semi-quantified with a visual scale that was used during the HSR-EPM Program [1]. A description of the scale is as follows:

0 - Nothing. No TCP.
1 - Very Light. One or two needles can be seen here and there.
2 - Light. Needles confined to common portions of sample, i.e. to the dendritic region.
3 - Moderate. A little less than moderately heavy.
4 - Moderate-Heavy. 'Chock-full' with TCP but needles are still confined regionally as in 2.
5 - Heavy. A heavy, even, and continuous distribution of TCP. No non-TCP afflicted islands.
6 - Very Heavy. Heavier than 5.
7 - Extremely Heavy. Extremely copious quantities.

Results and Discussion

Chemical Analyses

The EPM102 alloy modifications were designed to optimize Al and Co levels around those in the Baseline EPM102 alloy. Higher Al contents were believed to increase the creep strength but decrease the stability of the alloy, and lower Co contents were believed to increase the oxidation resistance and decrease the SRZ resistance of the alloy [1]. Thus, the aim was to vary the Al content between 5.45 and 5.85w/o and to vary Co from 14 to 17w/o. As seen in Table I and Figure 1, analyzed slab chemistries taken from each of the two molds of the same nominal alloy appear to be nearly identical for all alloys. The biggest deviation was seen in the analyzed Al content of EPM102C, but even that difference of 0.06w/o is within expected experimental scatter. These results suggest that the Al additions made to the master heats during casting were performed successfully for the two molds of the same alloy.

Figure 1 also indicates the proximity of each EPM102 alloy modification to the Baseline EPM102. It should be noted that the analyzed chemistry of EPM102A is statistically equivalent to that of Baseline EPM102 from a previous alloying campaign. Figure 1 displays the error bars based on 95% confidence intervals for the mean of seven repeat chemical analyses [6] that were performed on Baseline EPM102. The analyzed slab chemistries of EPM102A fall within the confidence intervals of Baseline EPM102, which indicates that EPM102A can be treated as compositionally identical to Baseline EPM102.

Creep Rupture Properties

Creep rupture tests were performed at a Pratt & Whitney vendor on uncoated specimens of each of the EPM102 alloy versions. As mentioned previously, the uncoated specimens received a full heat treatment prior to testing, which consisted of a 2050^{o}F/4-hour stress relief, a 16-hour simulated PtAl coating cycle, and a 1600^{o}F age for 12 hours. Duplicate creep rupture tests of uncoated specimens in this condition were conducted at 1800^{o}F and 45ksi on EPM102A, EPM102C, EPM102C+, and EPM102D+, and the data are shown in Table II. The creep-rupture lives that were generated on these alloy modifications were equal to or greater than the Baseline EPM102 data [1] from a prior round, even though EPM102A is compositionally identical to Baseline EPM102. Furthermore, the uncoated lives exhibited by EPM102C, EPM102C+, and EPM102D+ were as high or higher than any previous data generated on any alloy in the HSR-EPM Program [1].

Coated specimens were processed by GE Aircraft Engines for subsequent creep rupture testing at NASA GRC. This coated material included specimens that had been given the full heat treatment for direct comparison to the uncoated samples. The full heat treatment again consisted of a 2050^{o}F/4-hour stress-relief, the PtAl coating cycle, and a 1600^{o}F age for 12 hours. Selected specimens were also processed with a carburization treatment for SRZ reduction. Prior to the application of the PtAl coating, these selected samples were given either a 2-hour carburization treatment at 2000^{o}F with no prior stress relief, or a stress relief heat treatment of 2050^{o}F for 4 hours followed by a 2000^{o}F/2 hr carburization treatment. The reader is referred to the Materials and Procedures for further processing details on these particular specimens.

These coated specimens were then creep-rupture tested at NASA GRC at 1800^{o}F and 45ksi. Table III lists the creep rupture properties for the coated specimens along with their respective processing treatments, and Figure 2 graphically displays the lives for both the coated (filled bars) and uncoated (open bars) specimens. The dramatic decrease in life exhibited by the coated specimens is clearly evident in Figure 2. The coated lives were all similarly low whether the specimen had been given a stress relief, a carburization, or both the stress relief and the

carburization prior to PtAl-coating. The coated lives were on average only about 62% of the corresponding uncoated lives for these EPM alloys. Coated specimens given only the stress relief prior to PtAl coating exhibited lives that were 57% of the uncoated lives. These decreases in creep life observed after PtAl coating were similar in magnitude to those observed for the Round 4 alloys (EPM94 through EPM101) [6]. The debits in life for the Round 4 alloys were attributed to the formation of SRZ under the PtAl coating during creep testing [6].

Secondary Reaction Zone (SRZ)

The coated specimens of EPM102A-D+ were all examined after creep rupture testing for SRZ formation in an effort to explain the reduction in life after PtAl coating. This microstructural examination was performed on longitudinal and transverse sections of the specimen gage lengths using back-scattered SEM. SRZ has been observed to develop in EPM alloys [1,3,5,6] under the diffusion zone of the PtAl coating and is a three-phase constituent having a γ' matrix with TCP and stringers of γ [7]. A typical example of SRZ formation is shown in Figure 3 along with the general microstructure in the vicinity of the diffusion zone between the PtAl coating and the superalloy substrate.

Microstructural analysis of the EPM102 modifications revealed that there was very little SRZ in some coated alloys and highly variable amounts of SRZ in other coated alloys. The percentage of the specimen periphery that was covered with SRZ under the coating was measured and has been superimposed for each specimen on the bar chart of creep rupture life at 1800^{o}F/45ksi in Figure 4. The amount of SRZ in EPM102C and EPM102C+ was minimal, ranging from 0 to 4%, although the coated life was on average only 57% of the uncoated life. Thus, such minimal SRZ formation during creep in these specimens cannot account for the observed decrease in life after coating. In EPM102A and EPM102D+, the amount of SRZ was larger and more variable, ranging from 4 to 26% in EPM102A and from 6 to 49% in EPM102D+. Again the percent coverage of SRZ bears no relationship to the observed decrease in life.

The thickness of SRZ did not vary with increasing specimen coverage. The average SRZ thickness observed in this round of alloys was 0.002in. (51μm), and an average maximum thickness of 0.003in. (76μm) was seen. All coated specimens also had a light to moderate precipitation of TCP laths adjacent to the diffusion zone, similar to that in Figure 3. It is currently believed that SRZ formation reduces the load-bearing cross-section of the creep specimen [1,6]. However, the formation of SRZ in these specimens and their associated reductions in load-bearing cross-section do not explain the nearly 40% reduction in life observed after PtAl coating. A detailed microstructural investigation was therefore undertaken in an attempt to isolate what could be causing this decrease in properties after coating.

Microstructural Features in Coated and Uncoated Creep Specimens

The PtAl coating was examined to determine if there was anything different about this particular batch of coated specimens. The thickness and appearance of the coating was comparable to earlier runs [9]. The coating after creep rupture consisted of a mixture of β NiAl and γ' grains. A diffusion zone developed between the PtAl bondcoat and the superalloy substrate, as shown in Figure 3. The diffusion zone microstructure was also similar to PtAl-coated single crystals examined earlier in the HSR-EPM program [9]. The diffusion zone had a high volume fraction of TCP and carbides which tended to decorate the grain boundaries within that region. A line of porosity was sometimes observed along the PtAl-diffusion zone interface. These microstructural features of the diffusion zone are considered typical and are not believed to be responsible for the dramatic decrease in creep properties in the coated specimens.

Most of the coated specimens came from a different mold than the uncoated specimens of the same nominal composition, as seen by comparison of Tables II and III. Because of the potential of mold-to-mold variations, several microstructural features were examined. The initial γ' size and morphology were examined in selected samples prior to creep testing. Comparisons were made between fully heat treated, uncoated samples processed by Pratt & Whitney and fully heat treated, coated samples processed by GE Aircraft Engines. Only EPM102A and EPM102C+ could be compared in this way because of the limited number of as-processed, uncoated specimens that were made available to NASA GRC. Figures 5a and b represent the γ–γ' microstructures within a dendrite core for an uncoated EPM102A specimen processed by Pratt & Whitney and for a coated EPM102A specimen processed by GE Aircraft Engines, respectively. The γ' particles in both photomicrographs are fine and similar in size and have begun to align along [001] directions. These microstructures indicate little differences between the uncoated and coated specimens of EPM102A.

Figures 6a and b depict the γ–γ' microstructures within the dendrite cores of EPM102C+ in uncoated specimens processed by Pratt & Whitney and in coated specimens processed by GE Aircraft Engines, respectively. Numerous γ' particles have started to coalesce along [001] orientations in both specimens of EPM102C+, although many γ' particles are still discrete. However, it is again evident from the microstructures in Figure 6 that the uncoated and coated specimens have similar microstructures for the same alloy composition. Therefore, the heat treatments performed on the coated and uncoated specimens appear to have been conducted similarly, and the initial γ' size and morphology were not contributing factors in reducing the creep rupture lives after PtAl coating.

Any significant difference in the level of TCP precipitation after creep rupture testing between coated and uncoated specimens may suggest mold-to-mold variations in terms of composition, segregation, or pre-testing exposures. Longer creep exposures may also cause an increase in the amount of TCP precipitation relative to shorter creep exposures. Figure 7 superimposes the TCP level for the uncoated and coated specimens after creep rupture at 1800°F and 45ksi, based on a semi-quantitative visual scale from 0 to 7. As described in the Materials and Procedures, a TCP level of 0 indicates no TCP, and a level of 7 indicates copious precipitation of TCP. The TCP levels for the uncoated specimens were determined in the HSR-EPM Program by Pratt & Whitney and those for the coated specimens were determined at NASA GRC.

Figure 7 indicates that EPM102A developed the least amount of TCP precipitation during creep rupture testing, which is consistent with its low level of Al. EPM102C, EPM102C+, and EPM102D+ tended to have very light to light levels of TCP, all confined to the dendrite cores, in both the coated and uncoated specimens. Most of the time, the TCP level was constant between the coated and uncoated conditions, even though the rupture lives, or exposure times, differed by as much as a factor of 2. The exception was the uncoated specimen of EPM102C+, which had a life of 412 hr and a moderately heavy precipitation of TCP (level of 4). The longer rupture lives of the uncoated EPM102C+ specimens, and the fact that EPM102C+ had the highest level Al content making it more susceptible to TCP formation with increased exposures, may account for this additional TCP formation. In any event, it may be seen in Figure 7 that most of the EPM102 alloy modifications exhibited light precipitation of TCP in both the coated and uncoated specimens. As a result, it is believed that TCP precipitation also did not contribute to the observed decrease in life after coating.

The location of secondary cracking in the failed rupture samples was examined in metallographically polished, longitudinal sections of the specimen gage lengths. All coated specimens exhibited similar densities and locations of secondary cracking, irrespective of whether carburization was performed or not. In the coated specimens, secondary cracking was most prominent in areas closer to the fracture surface, as seen in Figure 8a. Secondary cracking occurred in the internal regions of the specimens, emanating from internal pores or large carbides in the interdendritic regions, Figure 8b. In specimens containing SRZ beneath the diffusion zone, secondary cracks were also observed along the incoherent boundary between the SRZ and superalloy matrix or within the SRZ colony itself, Figure 8c. The propensity to form these SRZ-associated cracks increased as the percentage of SRZ coverage increased. The cracks associated with the SRZ colonies were often longer than the cracks associated with internal porosity or carbides but were usually blunted at the superalloy-diffusion zone interface, unless located near the fracture surface where they extended through the diffusion zone or out to the surface. However, the cracks associated with SRZ extended only a short distance into the superalloy beneath the diffusion zone.

In addition, secondary cracking was examined at NASA GRC in the uncoated specimens creep rupture tested by the Pratt & Whitney vendor. Secondary cracking was again more frequently observed near the fracture surface, Figure 9a, and decreased as a function of distance from the primary fracture. Similar to the coated specimens, these uncoated specimens also had secondary cracks that emanated from internal porosity or large carbides in the interdendritic regions, Figure 9b. Sometimes small cracks were also observed in regions of internal SRZ that were present in the dendrite cores of uncoated EPM102C+ specimens. Surface cracks and local surface depressions were present in these uncoated specimens, as seen in Figure 9c, and these tended to be associated with a three-phase constituent that looked similar to SRZ colonies. Overall, there were no significant differences in cracking observed between coated and uncoated specimens or between carburized and non-carburized specimens.

Additional Uncoated Creep Rupture Tests

As discussed in previous sections, numerous microstructural features were examined at NASA GRC in an attempt to determine factors that could have contributed to the observed decrease in creep rupture life after the PtAl coating was applied. None of the microstructural features examined were found to be responsible for this decrease observed

after coating. As a result, two available uncoated specimens were creep rupture tested at NASA GRC in an effort to verify the uncoated properties generated at the Pratt & Whitney testing vendor. It should be emphasized that these uncoated specimens were fully processed and heat treated by Pratt & Whitney and then were subsequently tested at NASA GRC. Thus, these uncoated specimens should have been identical in microstructure to those tested by the Pratt & Whitney vendor.

Figure 10 includes the creep rupture lives for these two additional tests, which are represented by the rightmost open bars for the EPM102A and EPM102C+ alloys; the data are included in Table III as well. It is evident from this figure that the lives of the uncoated specimens of EPM102A and EPM102C+ tested at NASA GRC were comparable to the coated rupture lives of the same alloys, and were significantly lower than the uncoated lives generated at the Pratt & Whitney vendor. Note that the NASA GRC generated rupture life of EPM102A was closer to the lives for Baseline EPM102 than the average EPM102A life generated at the Pratt & Whitney vendor. This is an important distinction because EPM102A is compositionally equivalent to the Baseline EPM102, based on the Pratt & Whitney chemical analyses. Thus, NASA GRC was unable to verify the high rupture life of 449hr generated by the Pratt & Whitney vendor for uncoated EPM102A. Nor was NASA GRC able to verify the average rupture life of 412hr generated by the Pratt & Whitney vendor for uncoated EPM102C+.

Creep rupture tests of uncoated specimens of EPM102B+ and EPM102B++ were also performed at NASA GRC. Prior to testing, these uncoated specimens received a full heat treatment at NASA GRC, which consisted of a 2050^{o}F/4-hour stress relief, a 16hr simulated PtAl coating cycle, followed by an air cool, and a 1600^{o}F age for 12 hours. Duplicate creep rupture tests were conducted at 1800^{o}F and 45ksi. These data on EPM102B+ and EPM102B++ have been combined with the uncoated rupture lives of the other alloys in Figure 11 and have been included in Table III. The open bars in the figure represent the data generated at the Pratt & Whitney vendor, and the cross-hatched bars represent those generated at NASA GRC. The TCP levels have also been superimposed in this figure. The EPM102B+ and EPM102B++ data appeared consistent with the other testing data generated at NASA GRC, since the rupture lives increased slightly with increasing Al content until moderate TCP instability occurred. Thus, EPM102B+ had a higher life than EPM102A due to the higher Al content in EPM102B+. However, EPM102B++ appeared to have exceeded the TCP stability limit, which caused its rupture life to drop.

Thus, the uncoated specimens tested at NASA GRC provided internally consistent results. In addition, the single uncoated EPM102A test at NASA GRC is consistent with the Baseline EPM102 tests. Therefore, it appears likely that a testing variation between the coated specimens and the uncoated specimens has led to the difference observed between the coated and uncoated creep rupture lives. It would have been preferred to have tested more uncoated specimens of these compositions at NASA GRC, but very few uncoated specimens were available to NASA GRC at the end of the HSR-EPM Program, so additional testing could not be accomplished.

Another unexpected difference emerged between the uncoated specimens tested at NASA GRC and the uncoated specimens tested at the Pratt & Whitney vendor. A dramatic difference in the oxidation behavior is evident in Figure 12, where the as-tested surfaces of the specimens tested at the Pratt & Whitney vendor are compared to the as-tested surfaces of the specimens tested at NASA GRC. All uncoated specimens of the alloys tested at the Pratt & Whitney vendor exhibited a silvery surface after creep rupture in air and those tested in air at NASA GRC all had a charcoal gray surface. X-ray diffraction and electron dispersive spectroscopy (EDS) of the as-tested specimen surfaces have both indicated that the specimens tested at the Pratt & Whitney vendor developed Al_2O_3 as the primary oxide, whereas the primary oxide in the NASA GRC tested specimens was NiO. The reason for the difference in surface oxides could either be from: a) differences in heat treatments prior to testing, b) heat treatments that were unintentionally omitted, c) specimen handling differences that caused oxide removal or spallation, or d) the creep testing methods themselves. None of these explanations is entirely satisfactory, however. Presumably, Pratt & Whitney heat treated all of the uncoated specimens in argon under the same conditions, including the uncoated specimens tested at NASA GRC. Furthermore, both facilities performed the creep testing in air, and neither testing lab controls humidity which is known to encourage spallation. So, in the absence of additional specimens, the exact reasons for this behavior remain elusive.

Figures 13a and b show cross-sections of the oxides present after testing at the Pratt & Whitney vendor and at NASA GRC, respectively. The Al_2O_3 scale in Figure 13a was compact and had a maximum thickness of only about 0.00018in. (4.5μm) in the uncoated specimen of EPM102C that had a 513hr life. In contrast, the NiO in Figure 13b had an outer scale and an internal oxidation region; the total thickness of the oxide was about 0.0016in. (41μm) in

uncoated specimen of EPM102A that had a 232hr life. If the inner oxide region represents metal recession, then the loss of load-bearing cross-section may be expected to reduce uncoated creep life, but not by as much as that seen in the uncoated EPM102A specimen creep tested at NASA GRC (relative to that tested at the Pratt & Whitney vendor).

As a result, the presence of the Al_2O_3 scale on the Pratt & Whitney tested material does not explain the high lives reported for those uncoated specimens, and thus does not explain the dramatic reduction in rupture life that was observed in the coated specimens. The decrease in rupture life observed after PtAl-coating may not really represent a *coating debit* at all. Instead the difference in rupture lives between coated and uncoated specimens may be partially or substantially attributed to differences in the creep testing procedures used in each respective laboratory.

Efficacy of SRZ-Reduction Techniques in Creep Rupture Specimens

Figure 14 graphically displays the amount of SRZ observed under the PtAl coating in the creep specimens of the EPM102 alloy modifications. As stated in an earlier section, very little SRZ was observed in some coated alloys and highly variable amounts of SRZ were seen in others. The amount of SRZ in EPM102C and EPM102C+ was minimal after creep rupture, irrespective of the SRZ fix that was employed, and ranged from 0 to 4%. This was consistent with the low levels of SRZ that were reported along external surfaces of airfoil sections [1] of EPM102C and EPM102C+ after 1800°F isothermal exposures for 400 hr. Thus, EPM102C and EPM102C+ had a low propensity to form SRZ in both blades and creep specimens.

However, as seen in Figure 14, the amount of SRZ that formed in the creep specimens of EPM102A and EPM102D+ was larger and more variable than that observed in EPM102C and EPM102C+. Furthermore, the amount of SRZ in creep specimens of EPM102A and EPM102D+ differed significantly from that reported along external blade surfaces [1] of the same compositions when stress relief heat treatments were performed prior to PtAl coating. These external blade surfaces [1] of EPM102A exhibited an SRZ coverage of only 5% after an isothermal age of 400hr at 1800°F, compared to 22% SRZ in a stress relieved creep specimen with a rupture life of 207hr. An extensive 80% SRZ was observed in external blade surfaces [1] of EPM102D+ after a 400hr isothermal exposure at 1800°F, compared to 6 and 47% SRZ in stress relieved creep specimens having rupture lives of 261 and 231hr, respectively. Since chemistry as well as surface stresses are drivers for SRZ formation [7], more SRZ was expected to form in airfoils because of the higher surface stresses compared to those in creep specimens [10]. Thus, the higher amounts of SRZ observed in the creep specimens of EPM102A were difficult to rationalize. The widely divergent amounts of SRZ present in the creep specimens of EPM102D+ were also difficult to understand. One explanation may be handling differences during processing of the creep specimens where cold working or local stress concentrations introduced on the surface of the specimens could cause additional SRZ to form.

Another possibility for the high amounts of SRZ in the carburized specimens of EPM102A and EPM102D+ (Figure 14) may be ineffective carbon diffusion in the machined creep specimens during the carburization process. Microstructural observations made earlier in Baseline EPM102 [9] had shown that carburization reduced the amount of SRZ when carbon had diffused to sufficient depths such that fine-scale tantulum carbides (TaC) formed under the diffusion zone. However, examination of the EPM102A-D+ creep specimens after rupture at 1800°F and 45 ksi indicated that fine-scale tantulum carbides (TaC) were not present under the diffusion zone in the carburized specimens, including those specimens that exhibited low amounts (4%) of SRZ, Figure 15. Rhenium-rich TCP lath formation under the coating did occur beneath the diffusion zone. Thus, it appears possible that the carburization process was performed to insufficient depths into the substrate of these machined creep specimens.

Earlier studies on creep rupture of carburized EPM30 specimens indicated that some specimens failed in secondary creep and exhibited low lives and low reductions in area (RA) [1]. Statistical analyses [1] of these data showed high probabilities that carburization affected both rupture life and RA. Although high levels of carbon can embrittle nickel-base alloys, no microstructural evidence of significant quantities of carbon was found in the EPM30 samples [11]. In contrast, the creep rupture tests of EPM102A-D+ at 1800°F and 45ksi exhibited high RA with most specimens exhibiting RA greater than 20%, Figure 16. The lowest RA was exhibited by a single carburized specimen of EPM102C. However, when the RA of all the carburized specimens were pooled and compared to the RA of the pooled non-carburized specimens, no significant difference was observed in either the mean value of RA or in the range of RA. Figure 17 demonstrates this for the creep rupture data at 1800°F and 45ksi for EPM102A-D+. The final elongations are also shown in Figure 18 for the coated and uncoated specimens; all specimens showed greater than 15% elongation after creep rupture at 1800°F and 45ksi. All creep specimens failed

after extensive tertiary creep, including all of the coated specimens. Thus, low ductilities did not play a role in impacting the rupture lives of these EPM102 alloy modifications.

Interrupted Creep Tests

Creep tests were performed and interrupted prior to failure in order to examine the development of SRZ as a function of time during the creep test. No other interrupted creep tests had been conducted earlier during the HSR-EPM Program. The alloy selected for this study was EPM102D+ because a high amount of SRZ was expected to form under the coating. These tests were conducted in parallel with the microstructural analyses described earlier. The specimens were given the full heat treatment, consisting of a 2050°F/4-hour stress relief, the PtAl coating cycle, and a 1600°F age for 12 hours prior to creep testing. Figure 19 shows the creep curve for the 1800°F/45ksi test that was run to failure, and the amounts of SRZ and TCP measured as a function of time for the tests that were interrupted at 25, 80, and 159hr are superimposed on the figure. Unfortunately, the specimens all came from a mold that had developed an unexpectedly low amount of SRZ; only 6.3% of the specimen periphery was covered with SRZ under the PtAl coating after creep rupture. Thus, there was not a high level of SRZ development to examine as a function of time. It appeared that all the SRZ and TCP were present, within experimental scatter, after only 25 hrs of the creep test. It is possible that this SRZ was even present in the specimen prior to the start of the creep test, since earlier work [9] on EPM30 showed that a small amount of SRZ was sometimes present at the end of the high-temperature PtAl-coating cycle.

As discussed in an earlier section and seen in Figure 8c, secondary cracks were observed in creep ruptured specimens along the incoherent boundary between the SRZ and superalloy matrix or within the SRZ colony itself, when SRZ was present under the PtAl coating. However, the interrupted creep tests showed that the incoherent boundary surrounding the SRZ colony did not crack early in the creep test. In fact, in the creep test interrupted at 159hr and 2.7% strain, which was after the onset of tertiary creep, only one or two colonies of SRZ had cracks associated with them. The majority of SRZ colonies exhibited no cracking whatsoever. It is apparent that the cracking that is associated with the SRZ in the failed specimens occurred late in the creep test. Thus, the notion that the SRZ leads to premature cracking and early failure [5] is not consistent with the observations after interrupted creep.

Pre-Exposed Creep Specimens

Specimens of EPM102C and EPM102D+ were also given long-term, high temperature exposures prior to creep rupture testing in order to examine the effects of having a high amount of SRZ at the *start* of the test. The specimens were given the full heat treatment, consisting of a 2050°F/4-hour stress-relief, the PtAl (coated specimens) or simulated (uncoated specimens) coating cycle, and a 1600°F age for 12 hours, and then were aged for an additional 400hr at 2000°F. Creep rupture testing was conducted subsequently at 1800°F and 45ksi. Both coated and uncoated specimens were given this long-term 2000°F exposure. The long-term 2000°F exposure was expected to cause the formation of a high, equilibrium amount of SRZ in the coated specimens. For comparison, uncoated specimens of the same composition were also exposed for 2000°F for 400hr to produce the same starting γ-γ′ microstructure as that in the coated specimens, but with no SRZ.

Figure 20 is a bar chart of the uncoated creep lives for fully heat treated EPM102C and EPM102D+ and the lives of the specimens given the high temperature exposure of 2000°F for 400hr. It is evident from Figure 20 that both EPM102C and EPM102D+ exhibited lives that dropped precipitously after the 400hr age was given to either the coated or the uncoated specimen. Figure 21a indicates that the amounts of SRZ under the PtAl coating and internal TCP were higher than those that developed in the coated specimens without the extended exposure prior to creep rupture testing. Specifically, the coated and exposed specimens of EPM102C and EPM102D+ (mold 10) developed 14% and 18% SRZ, respectively, as compared to only 3% and 6% SRZ that formed in coated EPM102C and EPM102D+ (mold 10), respectively, which had been given no long-term aging prior to testing. Both alloys also exhibited higher levels of TCP of around 4 in the creep specimens with the extended exposure, as compared to a TCP level of 1 to 2 in the corresponding specimens without an extended exposure.

However, both the coated and uncoated specimens had developed an extremely coarsened γ-γ′ microstructure after the 2000°F/400hr exposure, Figure 21b, with the γ′ particles having coalesced along <001> directions prior to creep testing. This coarsened microstructure was not beneficial for creep resistance. Thus, to distinguish between the effects of TCP/SRZ instability and γ-γ′ microstructure, a single coated specimen of EPM102C that had been exposed for 400hr at 2000°F was subsequently resolutioned at 2400°F for 15minutes and then oil quenched. The

resolutioning treatment was expected to refine the initial γ′ size for improved creep properties without affecting the TCP and SRZ phases that had developed during the 2000°F exposure. The sample was then creep-rupture tested at 1800°F and 45ksi. Comparison of Figures 20 and 2 illustrates that the coated creep life was restored by at least 75% with this resolution treatment. Microstructural analysis revealed that the resolutioned specimen had extremely fine and discrete γ′ particles at the start of creep test and developed significantly finer rafted γ′ during creep-rupture compared to the 2000°F exposed material. The resolutioned sample maintained its moderately heavy TCP formation in the dendrite cores and its SRZ formation under the coating, and thus, these instabilities appeared unaffected by the 2400°F resolution treatment. It can be concluded that 1) the coarsened γ-γ′ microstructure was primarily responsible for the precipitous drop in creep life and 2) SRZ in modest amounts did not substantially affect the 1800°F creep properties.

Concluding Remarks

Debit after Coating

Significant effort was undertaken to determine the reason for the observed decrease in creep life in the coated EPM alloy modifications. Numerous microstructural features were examined, including:

- PtAl coating structure
- SRZ formation
- γ′ size and morphology
- internal TCP precipitation

None of these features contributed to the observed debit after coating. In addition, the amount of SRZ under the coating was not correlated with 1800°F creep life, and the interrupted creep experiments showed that the SRZ did not develop cracks until very late in the creep test, well after the onset of tertiary creep.

Therefore, the debit in creep properties observed after coating appears to have resulted from the use of different testing laboratories, with the uncoated specimens being tested at a Pratt & Whitney vendor and the coated specimens being tested at NASA GRC. It appears that testing variation at the two laboratories contributed to different creep properties observed in the coated and uncoated condition. This was further supported by the:

- lack of correlation of the vendor test results with the baseline EPM102 data
- good correlation between the uncoated GRC creep test with the baseline EPM102 data
- consistent GRC test results on uncoated EPM102A, EPM102B+, EPM102C+, and EPM102B++ specimens

If the uncoated properties are in fact closer to the coated properties, as the NASA GRC data suggest, the ultimate temperature capability of the uncoated EPM alloys would be significantly impacted. Figure 22 is a Larson Miller Parameter plot which compares coated and uncoated EPM102C data to various uncoated alloys, including the René N5/PWA 1484 data (2) which was used as a baseline in the EPM program. The René N5/PWA 1484 baseline data are represented by the long dashed lines between 45 and 22ksi in Figure 22. Creep rupture data obtained from the literature are also shown in Figure 22 for the second-generation single crystal superalloy René N5 (12) and third-generation single crystal superalloys René N6 (12) and CMSX-10Ri (13). Data curves only were presented in Reference 12, whereas the data points reported in Reference 13 are illustrated by the small, closed symbols in Figure 22. The limited rupture data generated during the EPM program on René N5 (2) appears to be significantly better than the René N5 data (12) obtained from the literature. Significant scatter in the CMSX-10Ri data is apparent, particularly in the stress range around 28ksi.

If the uncoated EPM102C rupture life at 45ksi is lower and approaches the coated EPM102C life, the temperature advantage of the EPM alloys over the average René N5/PWA 1484 baseline decreases at 45ksi from 75 to 50°F and approaches third-generation alloy performance. This is unfortunate since the improvement of the EPM alloys over the average René N5/PWA 1484 baseline appears to be greatest at the higher stress levels and at lower temperatures. The temperature advantage of these EPM alloys over the average René N5/PWA 1484 baseline is reduced further at lower stress levels and higher temperatures.

A majority of the uncoated specimens were also creep rupture tested at 2000°F during the HSR-EPM Program at the Pratt & Whitney vendor, and unfortunately only a few uncoated specimens are still available for 2000°F testing at NASA GRC. It is possible that NASA GRC may again be unable to verify the uncoated 2000°F creep properties generated at the vendor. The best approach to resolve this issue and to determine the response of the material after

PtAl coating is to conduct all the creep testing on coated *and* uncoated specimens at the same laboratory and using the same testing procedures. For this purpose, it is proposed that EPM102B+ and EPM102B++ be used since a sufficient number of specimens are still available for each of these two alloys. The results obtained will provide an accurate assessment of any coating debit in these alloys, since potential testing variation will be eliminated.

SRZ Variation

The variation observed in EPM102A and EPM102D+ in the amount of SRZ under the PtAl coating after creep rupture is not understood. Certainly a different composition would impact the amount of SRZ that develops, and thus the Al additions made to the master heats could be suspect. However, no Al additions were made to castings of EPM102A and all coated specimens of EPM102A came from the same mold. In contrast, the coated specimen of EPM102D+ that exhibited only 6% SRZ coverage came from a different mold than the other EPM102D+ specimens that had SRZ coverages ranging from 21 to 49%. The analyzed chemistries performed by Pratt & Whitney indicate no significant differences in chemistry between molds of the same alloy. So, at this time, the variation in the amount of SRZ observed within a single alloy is attributed to unanticipated differences in specimen handling or perhaps non-reproducibility in the specimen preparation for carburization or in the carburization treatment itself.

Considerable effort at GE Aircraft Engines and at NASA GRC has been focussed on understanding SRZ formation under the bondcoat. Although the effect of chemistry on SRZ formation is clearly recognized, the effect of surface stresses on SRZ formation has not been specifically addressed via systematic experiments. Certainly the SRZ formation appeared to have little impact on the 1800°F coated creep properties, since widely varying amounts of SRZ after creep rupture occurred in specimens with equivalent lives. The interrupted creep experiments also indicated that the effect of SRZ was minimal at 1800°F.

However, the impact of SRZ is expected to be greater in 2000°F creep where the SRZ thickness and extent of SRZ coverage is expected to be greater. Work that remains to be done in this area also includes examining the development of SRZ in specimens that form significant quantities of SRZ. Coated specimens given no SRZ reduction techniques should be examined during interrupted creep testing at 2000°F. A coated specimen of EPM102D+ (mold 10) without a stress relief developed about 20% SRZ after creep rupture at 1800°F and 45ksi, compared to 6% SRZ in those with a stress relief (also from mold 10). As a result, the potential exists for tracing the development of more significant quantities of SRZ in these alloys at 2000°F. It will also be useful to determine if the cracking associated with significantly higher quantities of SRZ continues to occur late in the creep test where its influence is minimal.

Optimization of γ′ Size

Although the initial γ-γ′ microstructures did not differ significantly between the coated and uncoated specimens of the same alloy, it was evident that the γ-γ′ microstructures of EPM102C+ and EPM102D+ were slightly overaged and not optimum for creep. The overaged microstructures resulted from the rather extensive, high temperature exposures prior to creep testing, which include the 4hr stress relief at 2050°F as well as the 16hr PtAl coating cycle at 1975°F. Optimization of the heat treatments for each alloy may further improve their respective creep properties. This notion is supported by the resolutionizing experiment that was performed which refined the γ′ size in coated EPM alloys after an extended age at 2000°F. The resolution treatment improved the creep rupture lives by a factor of six by refining the γ-γ′ microstructure without affecting the TCP or SRZ formation. Earlier studies on Round 1 EPM alloys [3] and first-generation nickel-base superalloys [14-17] also clearly demonstrated the potent role of an optimum, initial γ-γ′ microstructure on subsequent creep rupture properties.

Conclusions

1. SRZ formation did not significantly impact the creep rupture lives at 1800°F. This was evident from the widely varying amounts of SRZ in coated specimens and the equivalence of lives for those corresponding specimens.

2. The incoherent boundaries around the SRZ colonies under the PtAl coating do not crack until late in the creep test at 1800°F, well after the onset of tertiary creep and at strain levels greater than 3%. Thus, the effect of SRZ under the coating does not appear to be related to early cracking and premature failure as was suggested early [5] in the HSR-EPM Program.

3. It is not clear if there is an actual decrease in creep life in the EPM102 alloy modifications after PtAl coating. The observed decrease appears to be the result of conducting the coated and uncoated specimen tests at different testing laboratories. The true debit after coating will be determined in EPM102B+ or EPM102B++ in which all of the creep rupture testing on coated and uncoated specimens can be conducted at the same laboratory with identical testing procedures.

4. Because the high uncoated creep rupture lives generated on the EPM102 alloy modifications at the Pratt & Whitney vendor could not be substantiated at NASA GRC, the uncoated properties may be closer to the coated properties than previously thought. As a result, the temperature advantage of the EPM alloys over the average René N5/PWA 1484 baseline at 45ksi may be decreased from 75°F to 50°F.

References

1. Enabling Propulsion Materials Program: Final Technical Report, Volume 4, Task J - Long-Life Turbine Airfoil Material System, 01 October 1998 to 31 October 1999, NASA Contract NAS3-26385, May 2000.
2. Enabling Propulsion Materials Program: Annual Technical Report, Volume 3, Task C - Other Critical Components, 01 January 1993 to 31 December 1993, NASA Contract NAS3-26385, 31 January 1994.
3. Enabling Propulsion Materials Program: Annual Technical Report, Volume 5, Task J - Long-Life Turbine Airfoil Material System, 01 January 1994 to 01 May 1995, NASA Contract NAS3-26385, 25 June 1995.
4. Enabling Propulsion Materials Program: Annual Technical Report, Volume 4, Task J - Long-Life Turbine Airfoil Material System, 01 June 1995 to 30 September 1996, NASA Contract NAS3-26385, 30 November 1996.
5. Enabling Propulsion Materials Program: Annual Technical Report, Volume 4, Task J - Long-Life Turbine Airfoil Material System, 01 October 1996 to 30 September 1997, NASA Contract NAS3-26385, 31 January 1998.
6. Enabling Propulsion Materials Program: Annual Technical Report, Volume 4, Task J - Long-Life Turbine Airfoil Material System, 01 October 1997 to 30 September 1998, NASA Contract NAS3-26385, 30 November 1998.
7. W. S. Walston, J. C. Schaeffer, and W. H. Murphy, "A New Type of Microstructural Instability in Superalloys - SRZ," in Superalloys 1996, p. 9-18, R. D. Kissinger, et al., eds, The Minerals, Metals, and Materials Society, 1996.
8. ASTM Designation: E139-96, "Standard Test Methods for Conducting Creep, Creep-Rupture, and Stress-Rupture Tests of Metallic Materials, pp. 255-265, Volume 3.01 Metals- Mechanical Testing; Elevated and Low-Temperature Tests; Metallography, 1998 Annual Book of ASTM Standards, West Conshohocken, PA, 1988.
9. R. A. MacKay, A. Garg, and F. J. Ritzert, SRZ Designed Experiments, Presented at NASA-Glenn Research Center, September 23, 1999.
10. R. A. MacKay, SRZ Brainstorming Ideas, Presented at Pratt & Whitney Aircraft, April 22, 1998.
11. R. A. MacKay, A. Garg, D. Hull, and F. J. Ritzert, Studies on Current Carburization and Stress Relief Heat Treatment Processing, Presented at NASA-Glenn Research Center, March 29, 1999.
12. W. S. Walston, K. S. O'Hara, E.W. Ross, T. M. Pollack, and W. H. Murphy, "René N6: Third Generation Single Crystal Superalloy," in Superalloys 1996, p. 27-34, R. D. Kissinger, et al., eds, The Minerals, Metals, and Materials Society, 1996.
13. G. L. Erickson, U. S. Patent 5,366,695, "Single Crystal Nickel-Based Superalloy," 1994.
14. R. A. MacKay and L. J. Ebert, "Factors Which Influence Directional Coarsening of γ′ During Creep in Nickel-Base Superalloy Single Crystals," in Superalloys 1984, p. 135-144, M. Gell, et al., eds., The Metallurgical Society of AIME, 1984.
15. M. V. Nathal, "Effect of Initial Gamma Prime Size on the Elevated Temperature Creep Properties of Single Crystal Nickel Base Superalloys," Metall. Trans. A, Vol. 18A, 1987, pp. 1961-1970.
16. R. A. MacKay, M. V. Nathal, and D. D. Pearson, "Influence of Molybdenum on the Creep Properties of Nickel-Base Superalloy Single Crystals, Metall. Trans. A, Vol. 21A, 1990, pp. 381-388.
17. R. A. MacKay, Alternate Heat Treatments for Single Crystal Alloys, Presented at NASA Glenn Research Center, May 1, 1995.

TABLE I.—CHEMICAL ANALYSIS OF MASTER MELTS AND SLAB CASTINGS OF EPM102 ALLOYS (refs. 1 and 6)

Alloy	Chemistry	Weight %											ppm
		Cr	Mo	W	Re	Ru	Ta	Al	Co	B	C	Hf	Y
102A	Aim	2	2	6	6	3	8	5.45	16	0.004	0.03	0.15	
724Z33545 Master Heat	Analyzed	2.02	2.11	5.93	5.86	2.97	7.83	5.39	16.3	0.004	0.033	0.16	
102A Slab 21/ Mold 3	Analyzed	2.03	1.97	6.08	6.01	2.99	7.94	5.39	16.1	0.004	0.027	0.16	120
102A Slab 31/ Mold 4	Analyzed	2.03	1.97	6	5.91	2.92	8.04	5.39	16.1	0.004	0.029	0.16	130
102B	Aim	2	2	6	6	3	8	5.55	17	0.004	0.03	0.15	
725Z33546 Master Heat	Analyzed	2	2.1	5.91	5.87	3	8.23	5.43	16.95	0.004	0.036	0.15	
102B+Slab/ Mold 1	Analyzed	1.93	1.94	6	6.01	2.93	8.38	5.76	16.94	0.005	0.023	0.14	180
102B++Slab/ Mold 2	Analyzed	1.93	1.94	6.02	6.03	2.99	8.41	5.86	16.92	0.005	0.021	0.15	210
102C	Aim	2	2	6	6	3	8	5.7	17	0.004	0.03	0.15	
726Z33548 Master Heat	Analyzed	2.03	2.1	6.03	5.84	2.86	8.2	5.49	16.84	0.004	0.035	0.15	
102C Slab 42/ Mold 5	Analyzed	2.02	1.95	6.09	5.96	2.96	8.47	5.56	16.91	0.004	0.032	0.15	100
102C Slab 61/ Mold 6	Analyzed	1.88	1.96	6.03	5.92	3.01	8.62	5.62	16.91	0.004	0.027	0.16	100
102C+0.21Al Slab 72/ Mold 7	Analyzed	1.9	1.95	6.04	5.91	3.01	8.5	5.82	16.85	0.004	0.029	0.15	80
102C+0.21Al Slab 84/ Mold 8	Analyzed	1.9	1.95	6.02	5.91	3.01	8.55	5.81	16.84	0.004	0.029	0.16	90
102D	Aim	2	2	6	6	3	8	5.7	14	0.004	0.03	0.15	
727Z33547 Master Heat	Analyzed	2.03	2.1	5.94	5.91	2.83	7.96	5.44	13.93	0.004	0.031	0.15	
102D+0.16Al Slab 51/ Mold 10	Analyzed	2.02	1.97	6.08	5.93	2.93	8.16	5.68	13.94	0.003	0.027	0.15	60
102D+0.16Al Slab 95/ Mold 9	Analyzed	1.91	1.96	6.09	5.97	2.91	8.16	5.67	13.95	0.003	0.024	0.16	110
Baseline 102	Aim	2	2	6	6	3	8	5.6	16	0.004	0.03	0.15	
Master Heat	Analyzed	2.1	2.1	6.1	6.1	3	8.3	5.6	16	0.0038	0.051	0.16	
Average of 7 Slab Samples	Analyzed	2	2.06	6	5.9	2.91	7.94	5.44	16.11	0.0038		0.14	144

TABLE II.—SUMMARY OF PRATT & WHITNEY CREEP-RUPTURE DATA FOR UNCOATED EPM102 ALLOY MODIFICATIONS (ref. 1)

Alloy	Test condition	Specimen number	Mold number	Rupture life, hr	Time to 1 percent creep, hr	Time to 2 percent creep, hr	Elongation, percent
102A	1800°F/45ksi	28B1	3	275.0	177	203	15.2
		28T1	3	449.3	199	264	28.0
102C	1800°F/45ksi	46B1	5	488.2	312	343	34.6
		46T1	5	513.4	315	350	n/a
102C+	1800°F/45ksi	86B1	8	410.7	271	298	28.3
		86T1	8	412.5	280	307	21.4
102D+	1800°F/45ksi	57B1	10	418.9	284	316	n/a
		58T1	10	396.4	255	281	21.1
Baseline 102	1800°F/45ksi			279.5	162	182	20.0
				250.9	135	158	17.3

TABLE III.—SUMMARY OF NASA GLENN CREEP-RUPTURE DATA FOR COATED AND UNCOATED EPM102 ALLOY MODIFICATIONS

Alloy	Test condition	Specimen number	Mold number	2050°F/ 4 hr stress relief	Carburization	PtAl coating	Simulated coating cycle	1600°F 12 hr age	Rupture life, hr	Time to 1 percent creep, hr	Time to 2 percent. creep, hr	Elongation, percent
102A	1800F/45ksi	37-6	4	√	n/a	√	n/a	√	206.6	107	128	22.5
		40-1	4	n/a	√	√	n/a	√	240.6	129	151	21.9
		40-4	4	√	√	√	n/a	√	231.9	129	151	20.0
		40-6	4	√	√	√	n/a	√	235.3	119	141	25.6
		36T1	4	√	n/a	n/a	√	√	231.6	128	150	16.1
102C	1800F/45ksi	66-2	6	n/a	√	√	n/a	√	313.1	110	147	24.8
		66-6	6	√	√	√	n/a	√	284.3	176	196	25.4
		70-EX	6	√	√	√	n/a	√	287.7	173	192	29.0
		70-4	6	√	n/a	√	√	√	266.9	159	180	26.7
102C+	1800F/45ksi	80-3	7	√	n/a	√	n/a	√	254.7	159	179	24.4
		76-3	7	√	√	√	n/a	√	259.7	148	169	27.3
		76-5	7	√	√	√	n/a	√	252.6	153	170	23.6
		80-EX	7	n/a	√	√	n/a	√	298.0	206	229	17.1
		90T1	8	√	n/a	n/a	√	√	325.2	214	234	28.5
102D+	1800F/45ksi	97-5	9	√	n/a	√	n/a	√	231.0	128	148	29.0
		97-4	9	n/a	√	√	n/a	√	304.9	205	224	27.2
		100-2	9	n/a	√	√	n/a	√	263.3	166	185	24.3
		100-5	9	√	√	√	n/a	√	257.5	152	171	26.2
		58B6	10	√	n/a	√	n/a	√	261.1	158	178	28.1
102B+	1800F/45ksi	7-1	1	√	n/a	n/a	√	√	323.4	218	241	18.5
		7-4	1	√	n/a	n/a	√	√	287.4	190	211	15.0
102B++	1800F/45ksi	16-1	2	√	n/a	n/a	√	√	271.4	187	209	15.0
		16-4	2	√	n/a	n/a	√	√	254.0	167	187	17.8

n/a= not applicable
√ = applied

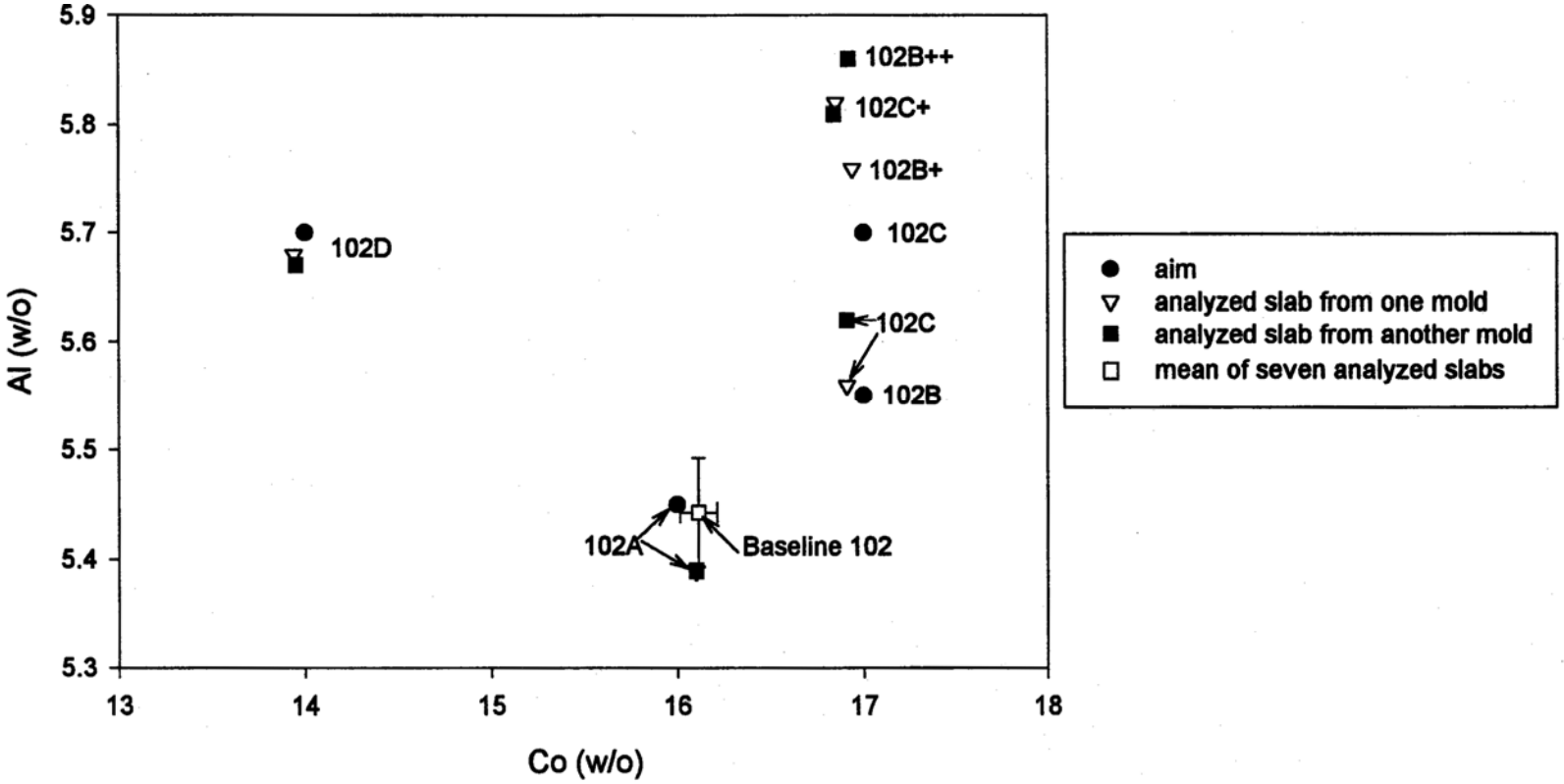

Figure 1. Compositions of slabs, analyzed by Pratt & Whitney [data from Refs. 1 and 6], along with desired aim compositions for EPM alloys. When two molds of slabs were cast for a given alloy, one slab from each mold was analyzed. Error bars for 95% confidence intervals for the mean of seven analyses are also shown for Baseline EPM102.

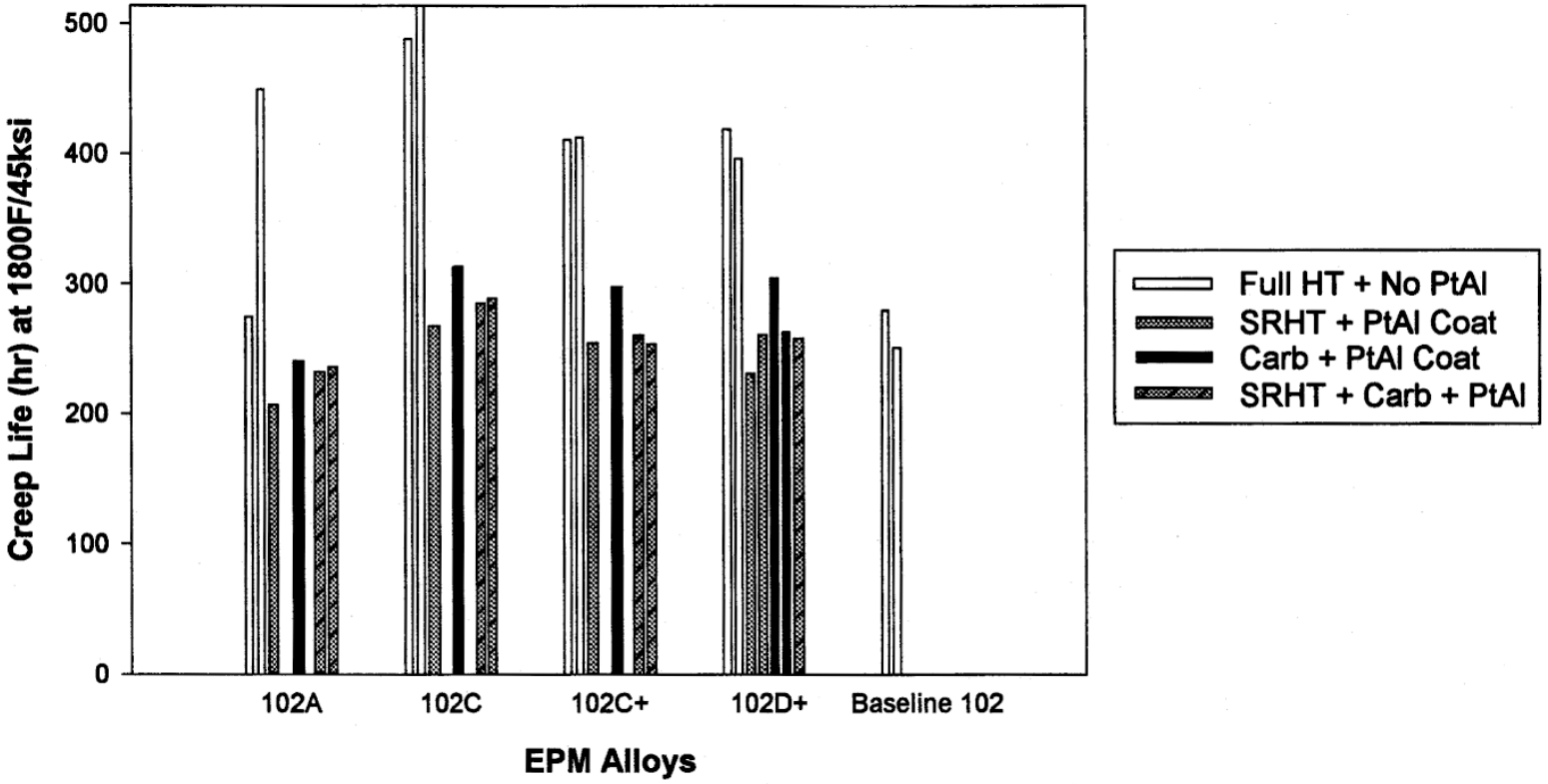

Figure 2. Creep rupture lives at 1800°F and 45ksi for uncoated and PtAl-coated EPM alloys. Uncoated specimens (open bars) were given a full heat treatment (HT) consisting of a stress relief heat treatment (SRHT), a simulated coating cycle, and a 1600°F age. Coated specimens (various filled bars) were given either a SRHT, a carburization treatment, or both the SRHT and carburization treatment prior to PtAl coating. All coated specimens also received the 1600°F post coating treatment.

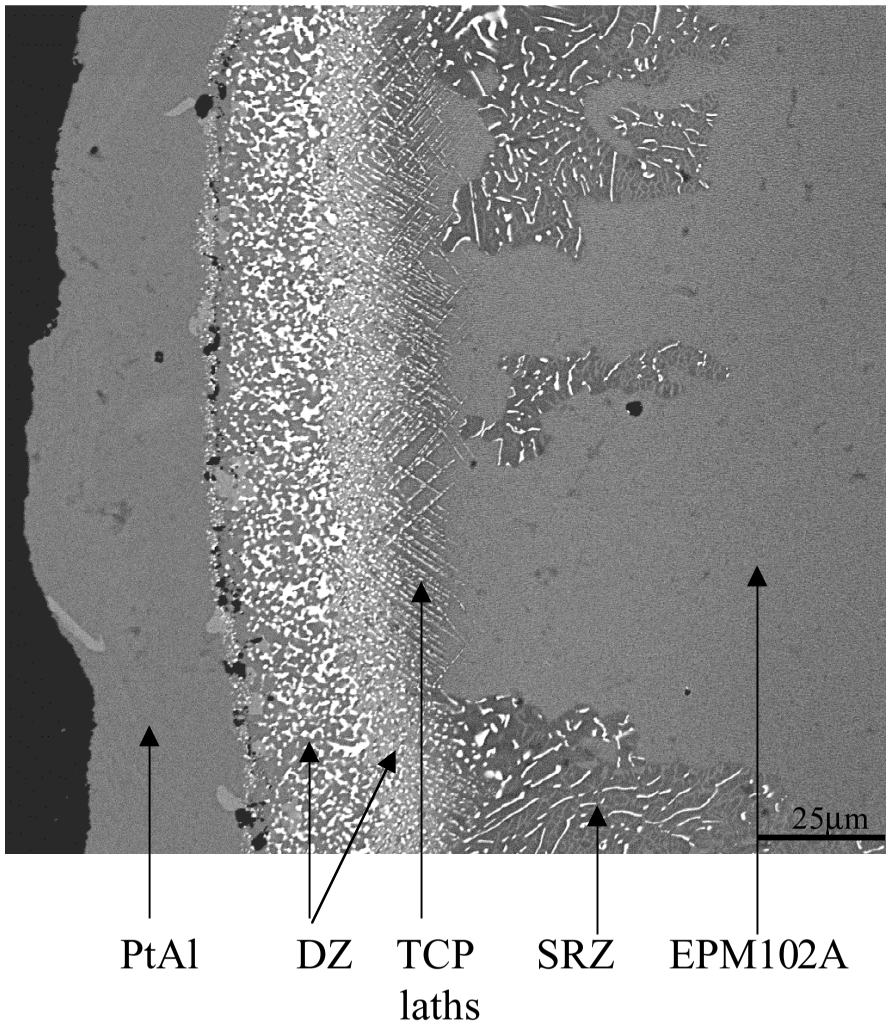

Figure 3. Secondary reaction zone (SRZ) formation is shown beneath the diffusion zone (DZ) of PtAl-coated specimen of EPM102A. The SRZ is a three-phase constituent consisting of a γ′ matrix with TCP and stringers of γ. TCP laths are also evident in a layer directly beneath the diffusion zone.

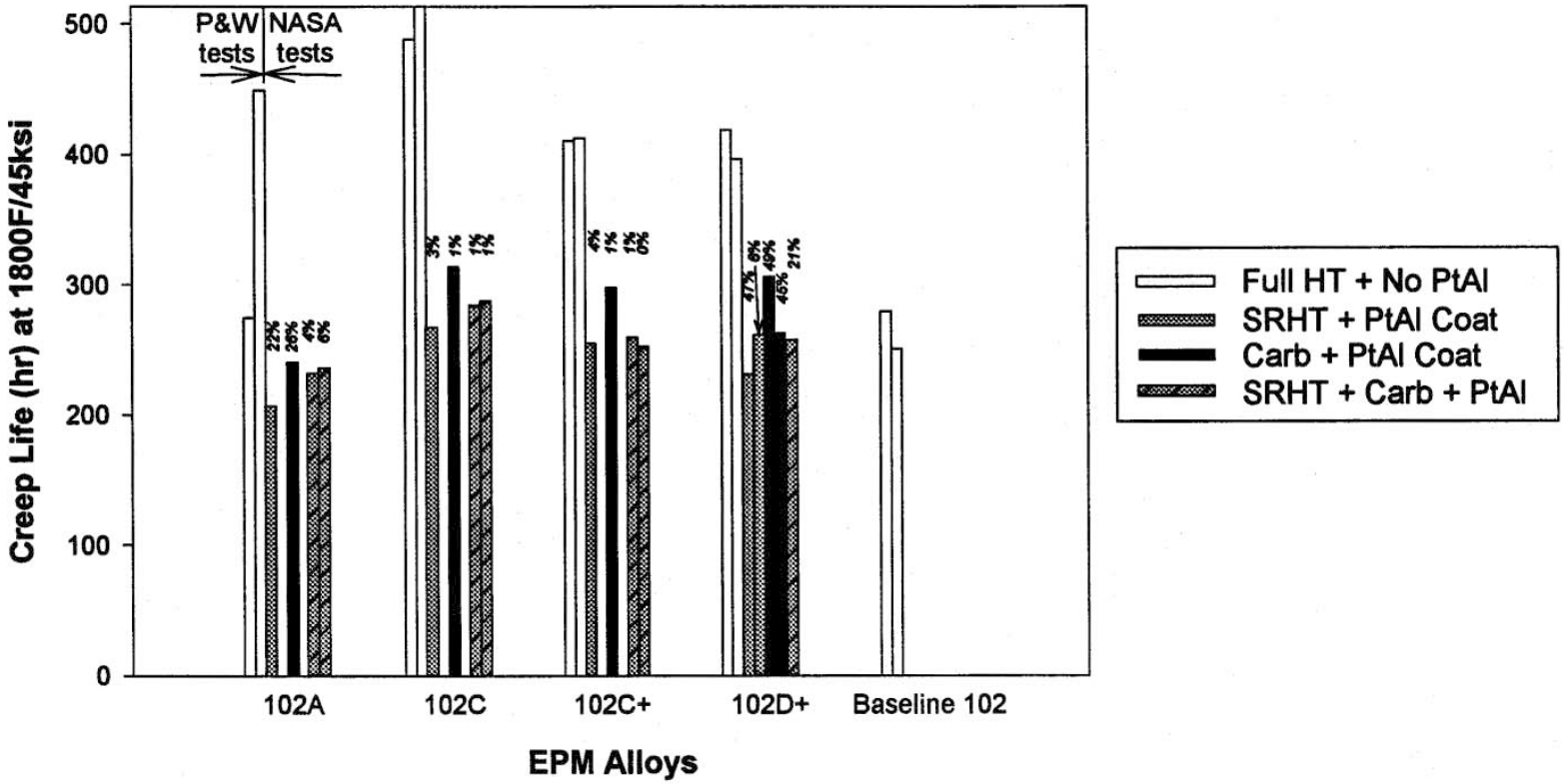

Figure 4. Uncoated and PtAl-coated creep rupture lives for tests at 1800°F and 45 ksi. The open bars represent uncoated specimens; filled bars represent coated specimens with various SRZ-reduction treatments. The first two bars for each alloy represent test results from a P&W vendor; the remaining bars for each alloy represent test results generated at NASA GRC. The two bars for the Baseline 102 alloy represent test results from a P&W vendor.

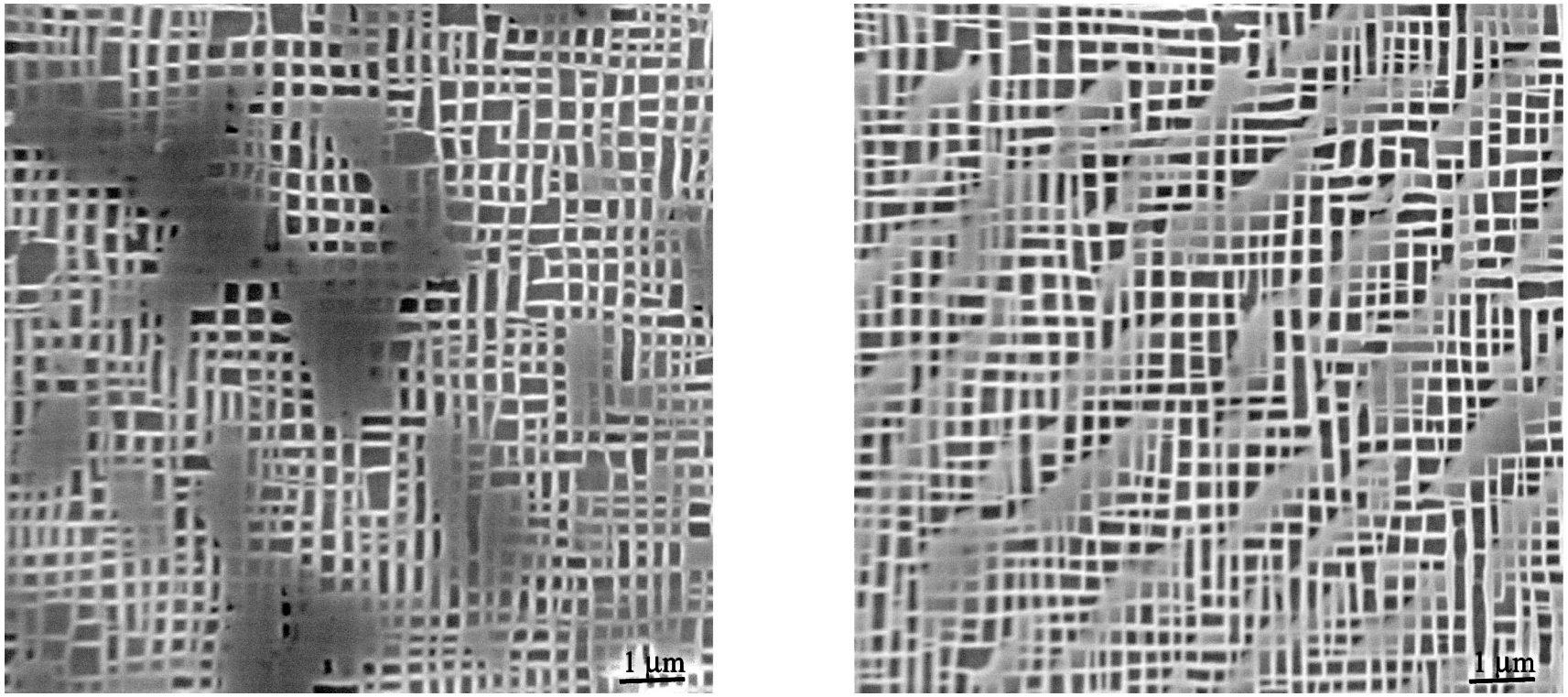

(a) (b)

Figure 5. As-processed γ-γ' microstructures in a dendrite core of EPM102A prior to creep rupture testing in (a) an uncoated specimen processed by Pratt & Whitney and in (b) a coated specimen processed by GEAE.

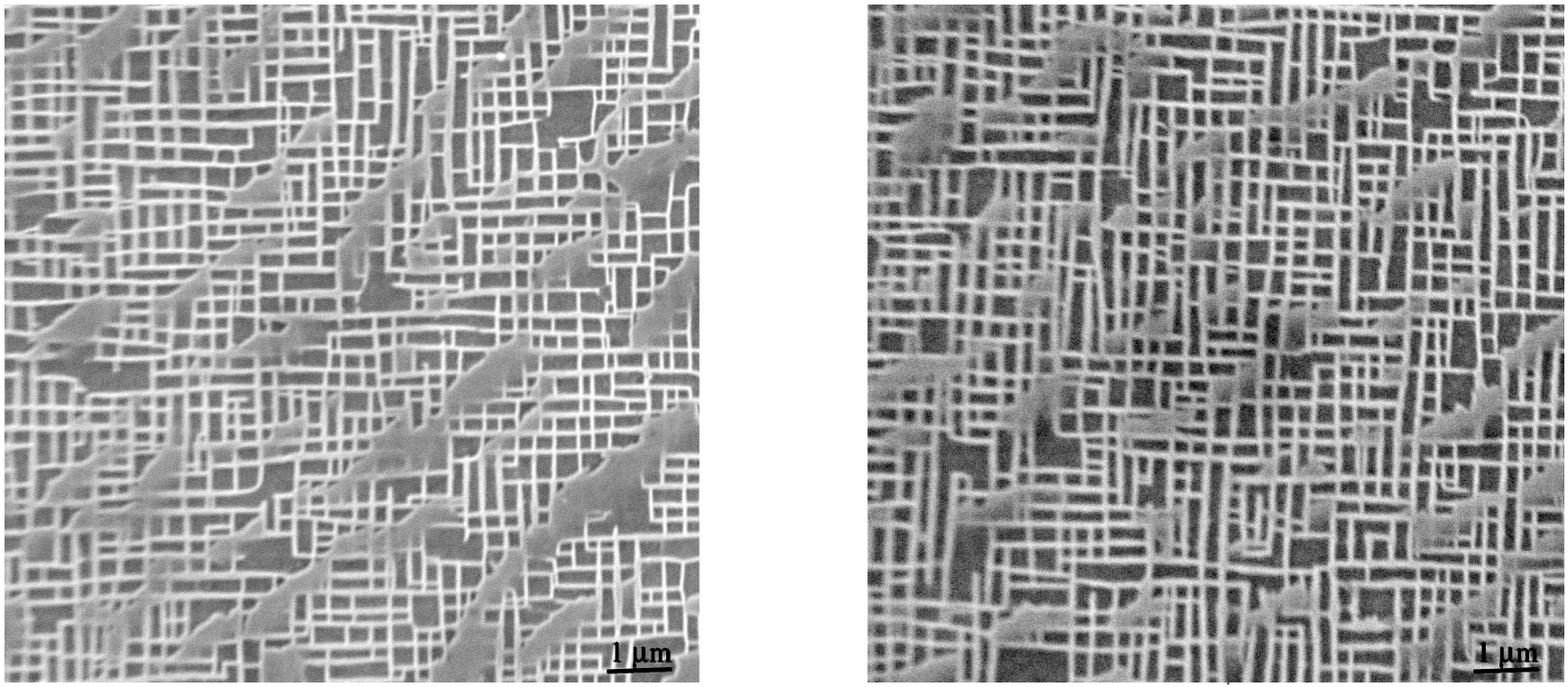

(a) (b)

Figure 6. As-processed γ-γ' microstructures in a dendrite core of EPM102C+ prior to creep rupture testing in (a) an uncoated specimen processed by Pratt & Whitney and in (b) coated specimen processed by GEAE.

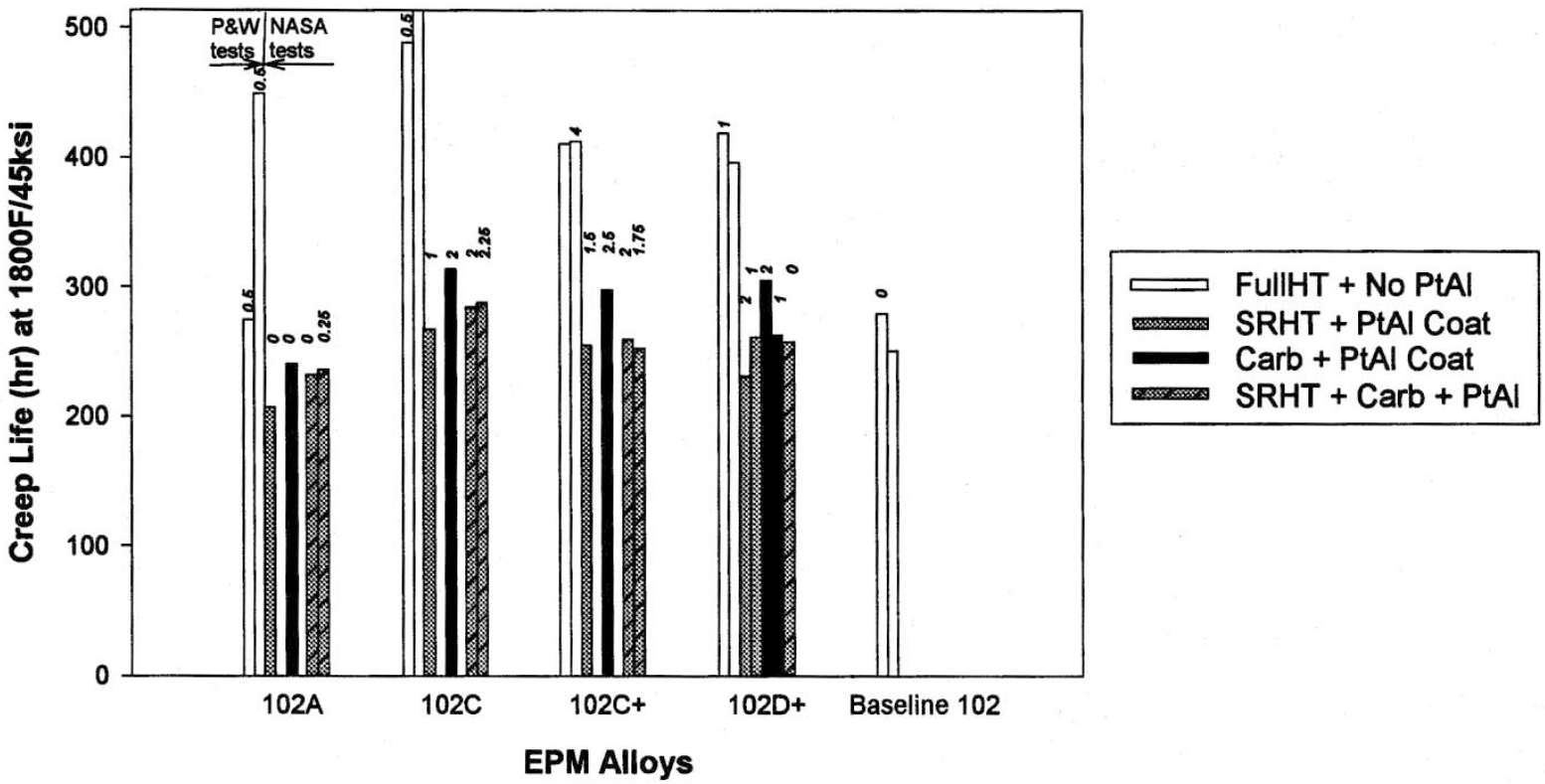

Figure 7. TCP precipitation levels superimposed above the creep rupture lives of uncoated specimens tested by a Pratt & Whitney vendor and for PtAl-coated specimens tested at NASA GRC. TCP levels were measured by Pratt & Whitney on the uncoated specimens. TCP levels in coated specimens were measured by NASA GRC.

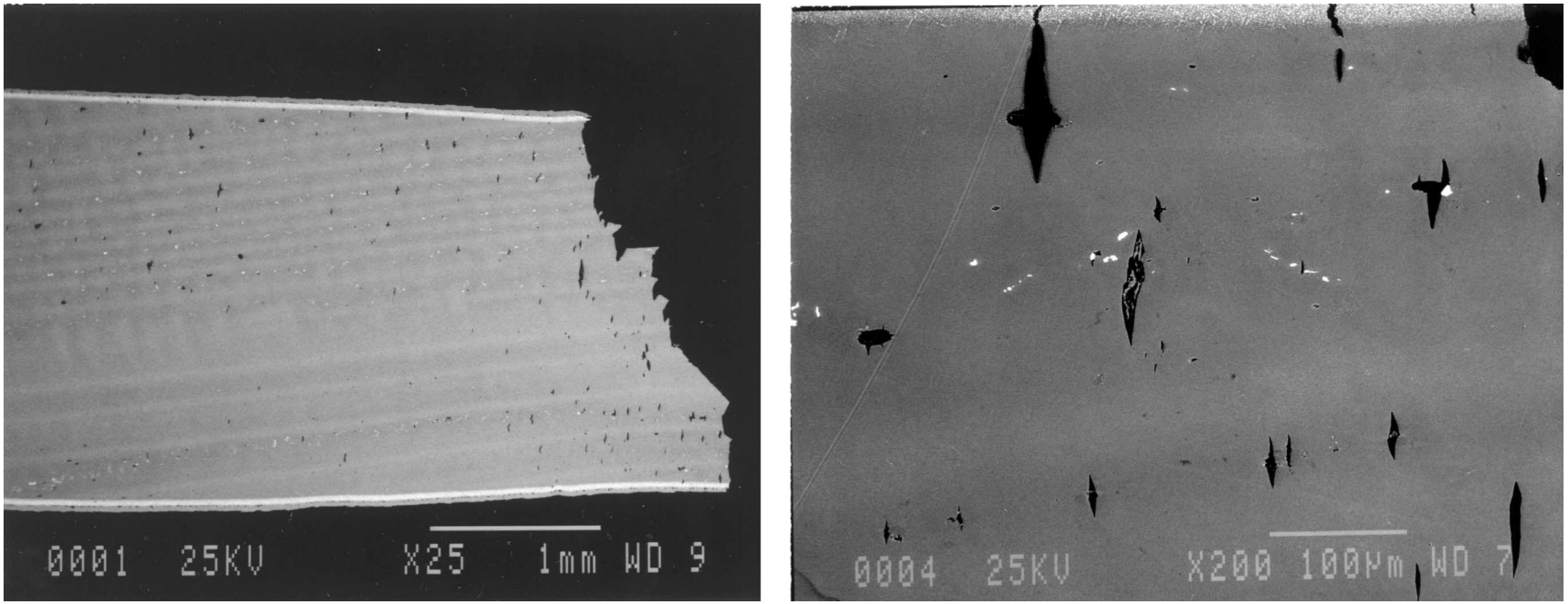

(a) (b)

Figure 8. Typical examples of secondary cracking in coated specimens of EPM102 modifications after creep rupture at 1800°F/45ksi. (a) Longitudinal section in vicinity of fracture surface where most of the secondary cracking occurred internally at pores or carbides. (b) Higher magnification showing secondary cracking in longitudinal section near fracture surface. Stress axis is horizontal.

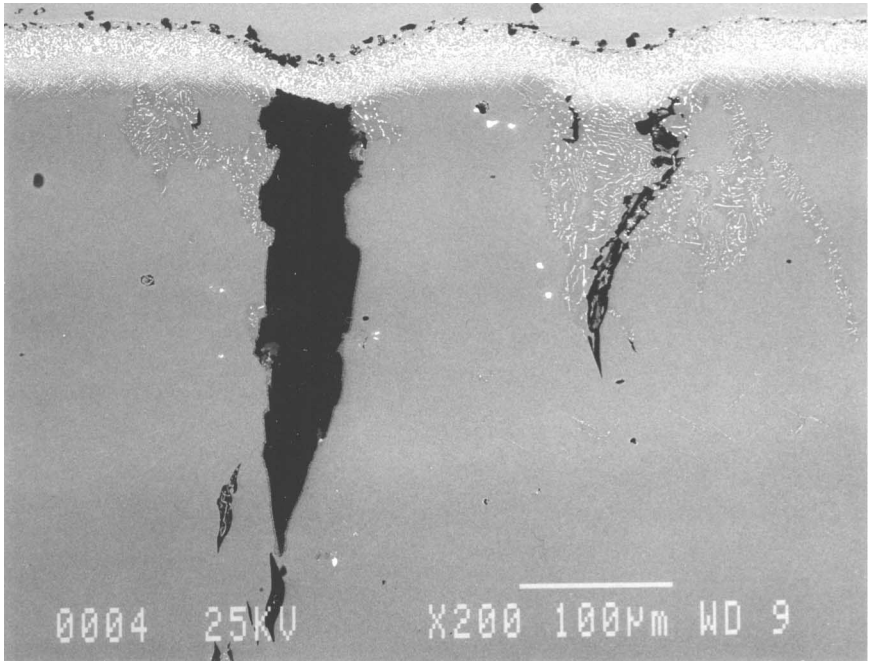

Figure 8(c). Secondary cracking associated with SRZ in coated EPM102C+ after creep rupture at 1800°F/45ksi. Stress axis is horizontal.

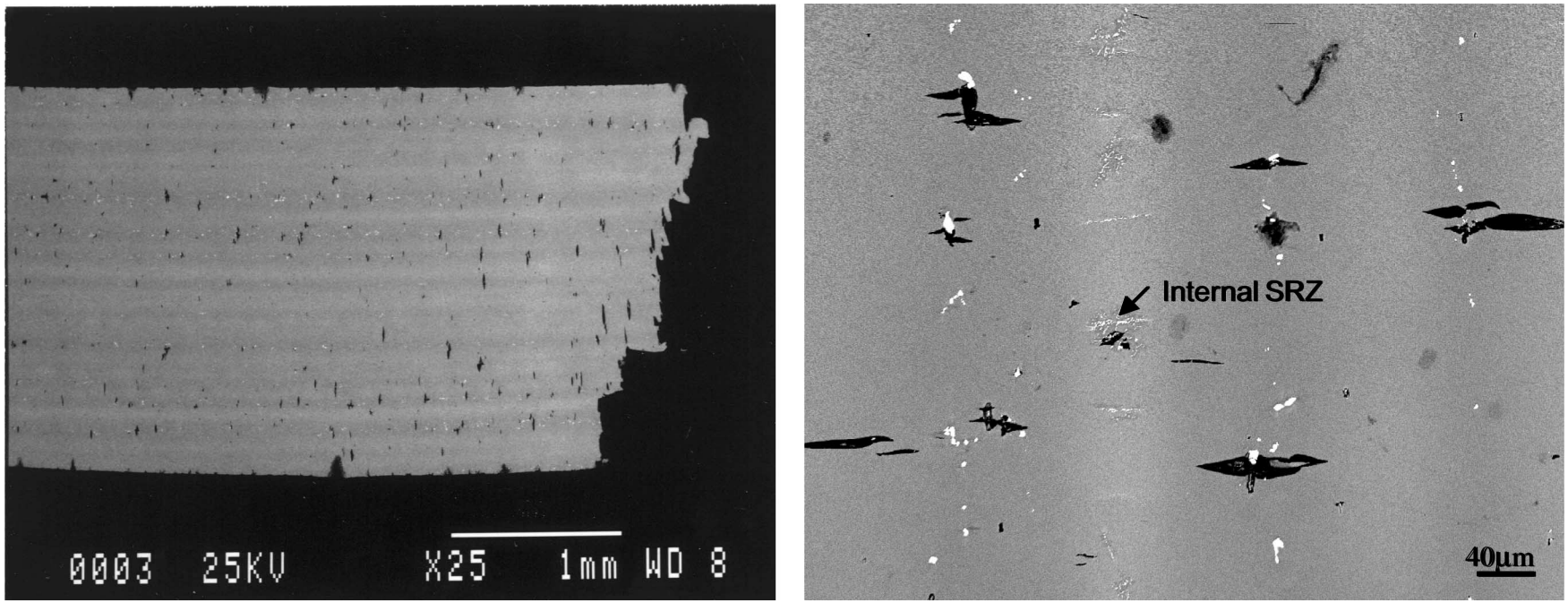

(a) (b)

Figure 9. Secondary cracking in uncoated specimens of EPM102 modifications after creep rupture at 1800°F/45ksi. (a) Longitudinal section in vicinity of fracture surface. Stress axis is horizontal. (b) Higher magnification showing secondary cracking at internal pores or carbides in longitudinal section near fracture surface. Cracks sometimes observed within dendrite cores in specimens containing regions of internal SRZ. Stress axis is vertical.

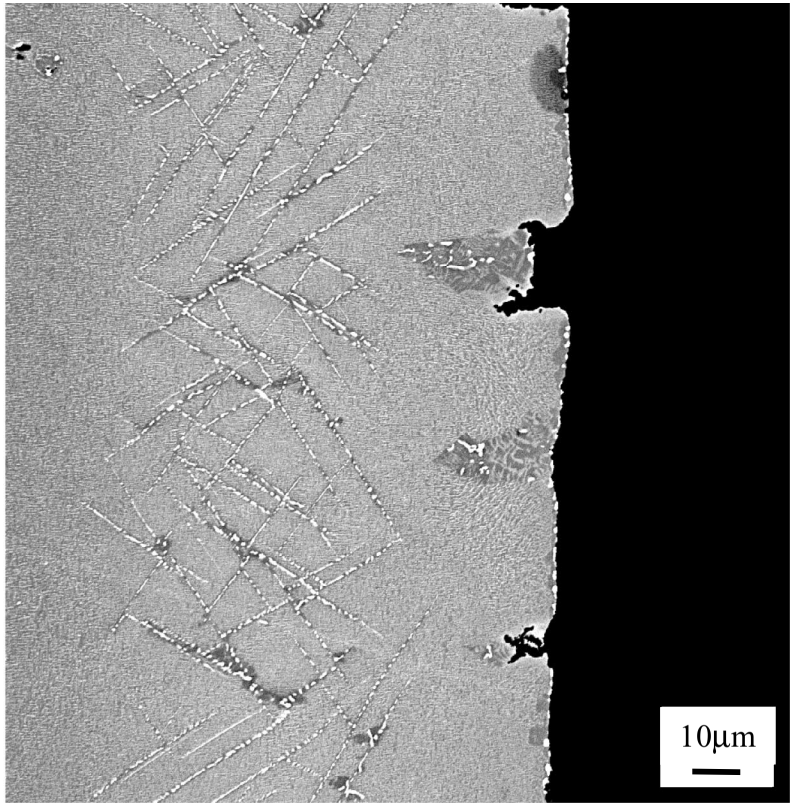

(c)

Figure 9(c). Surface cracks and local depressions present in uncoated specimens after creep rupture at 1800°F/45ksi. Stress axis is vertical.

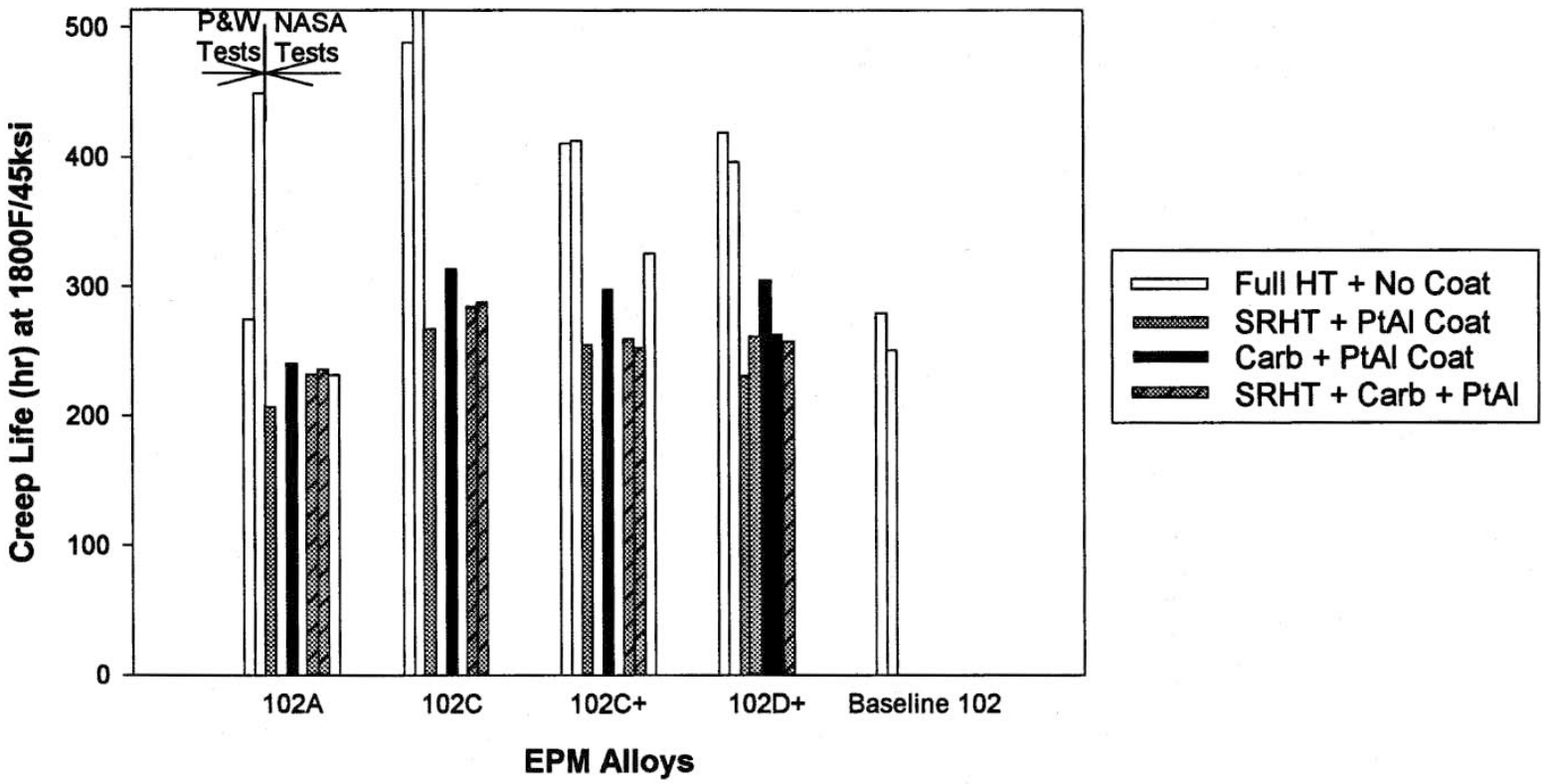

Figure 10. Uncoated and PtAl-coated creep rupture lives for tests at 1800°F and 45 ksi. The open bars represent uncoated specimens; filled bars represent coated specimens with various SRZ-reduction treatments. The first two bars for each alloy represent test results from a P&W vendor; the remaining bars for each alloy represent test results generated at NASA GRC. The two bars for the Baseline 102 alloy represent test results from a P&W vendor.

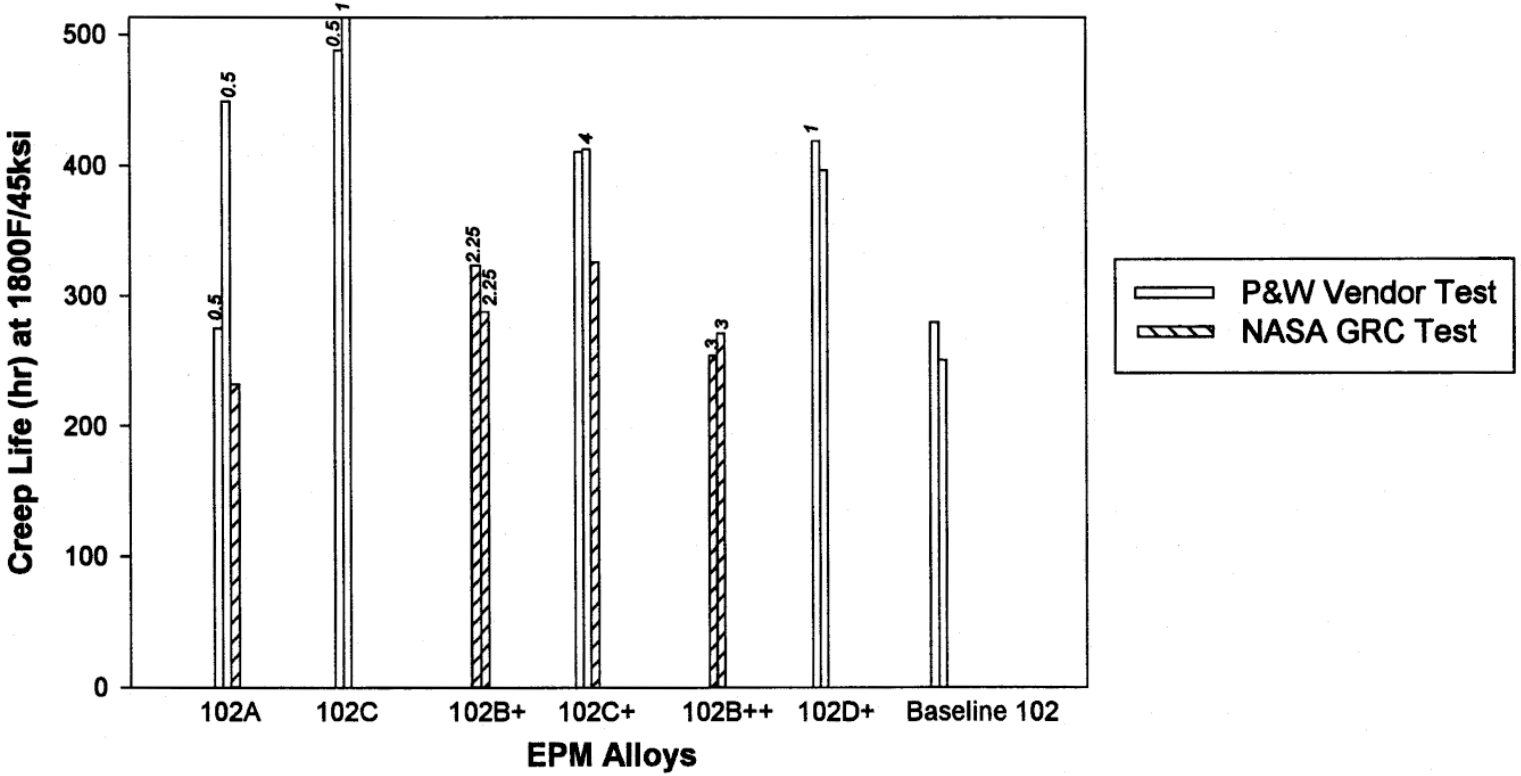

Figure 11. Uncoated creep-rupture lives for tests at 1800°F and 45 ksi. Tests were conducted at a Pratt & Whitney vendor (open bars) and at NASA GRC (hatched bars). TCP levels from a possible low of 0 to a possible high of 7 are superimposed above the bars.

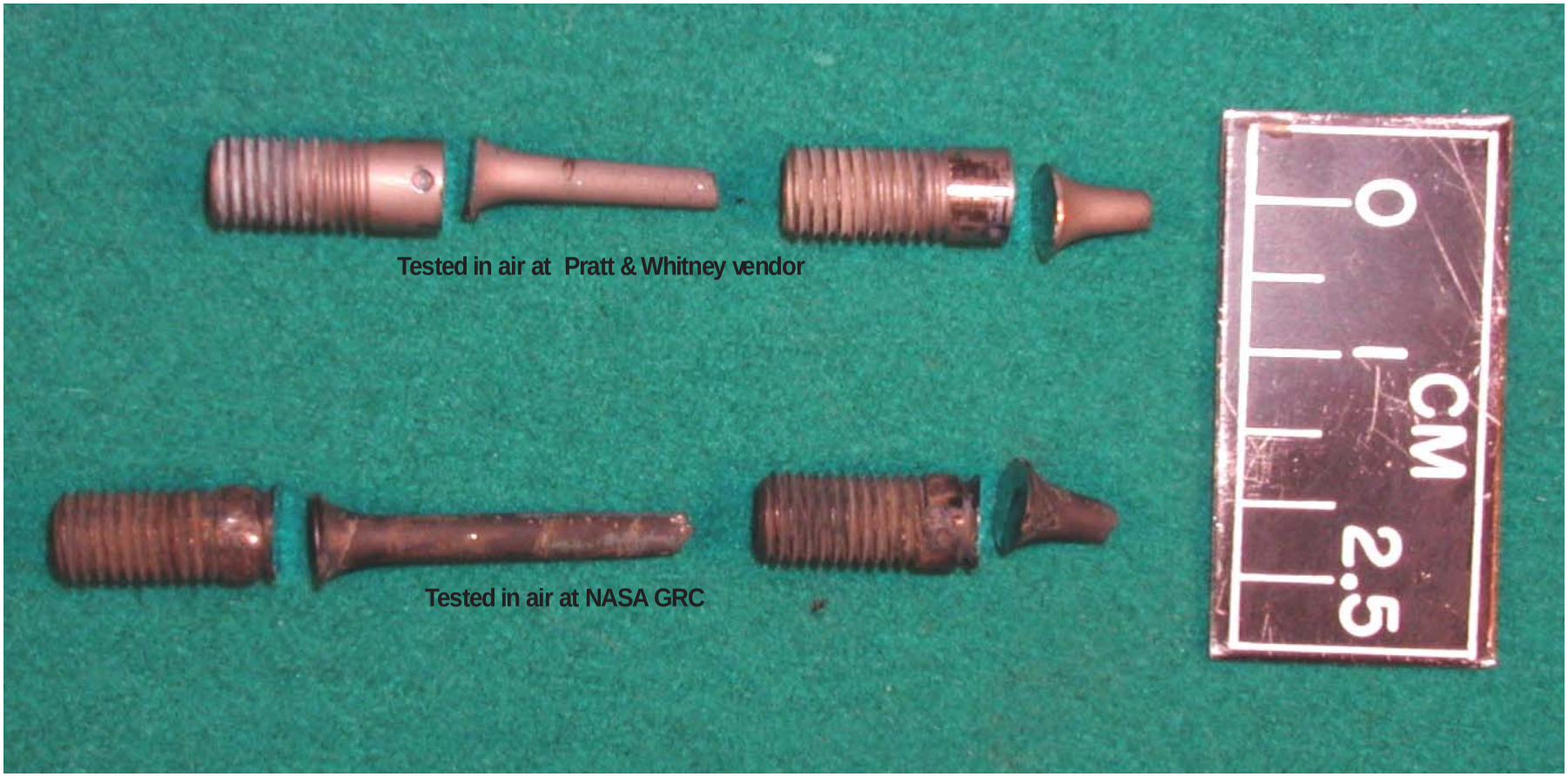

Figure 12. Comparison of as-tested surfaces of uncoated specimens of EPM102A after creep rupture testing in air at 1800 ˚F and 45 ksi. Both specimens were heat treated by Pratt & Whitney. However, the top specimen was creep rupture tested at a Pratt and Whitney vendor and had a 449 hr life; the bottom specimen was tested at GRC and had a 232 hr life.

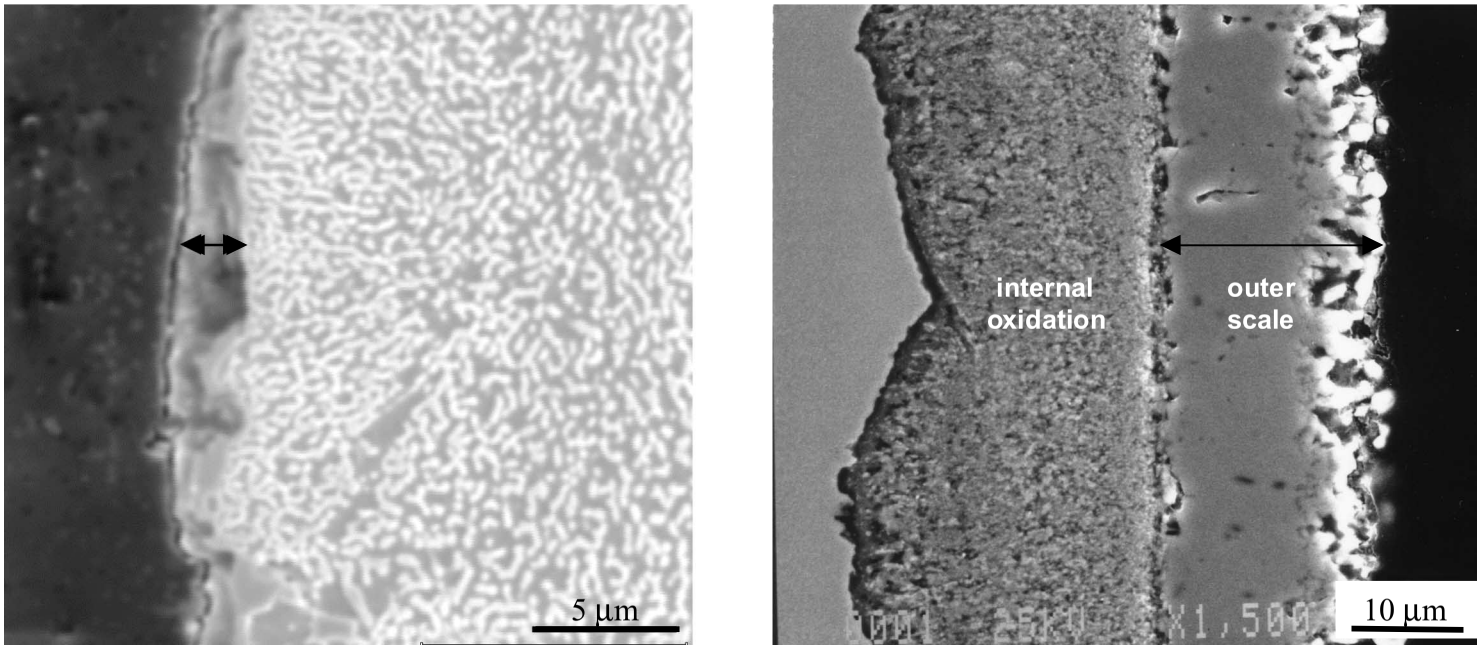

(a) (b)

Figure 13. Oxide scales present after 1800°F/45ksi creep testing at: (a) a Pratt & Whitney vendor and (b) NASA GRC. A thin scale of Al_2O_3 formed in (a), whereas the primary oxide was NiO in (b). Arrows depict the thickness of the outer oxide scales.

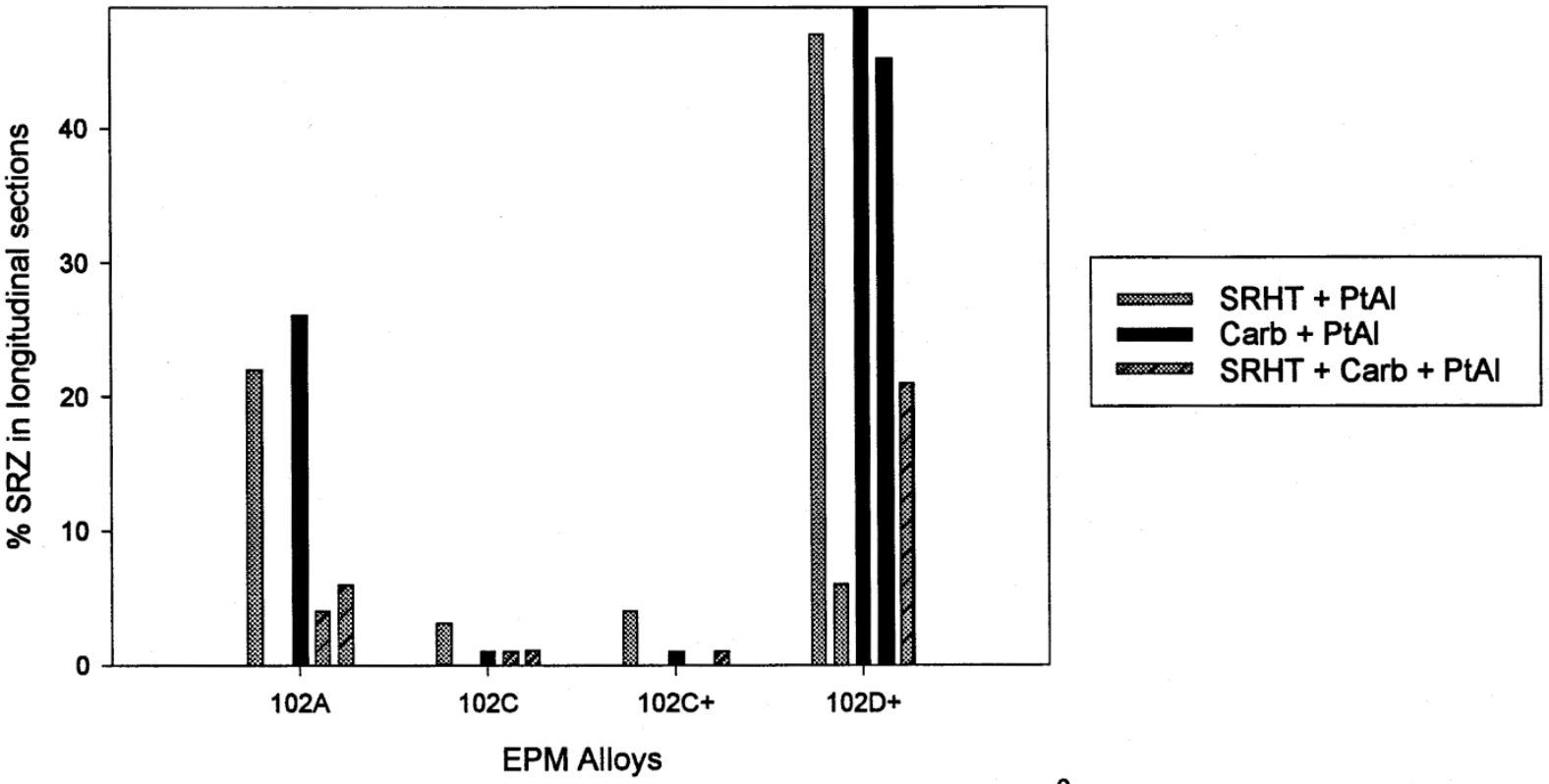

Figure 14. Amount of SRZ present in coated creep rupture specimens after failure at 1800°F and 45ksi. The filled bars represent coated specimens with various SRZ-reduction treatments. All tests were conducted at NASA GRC.

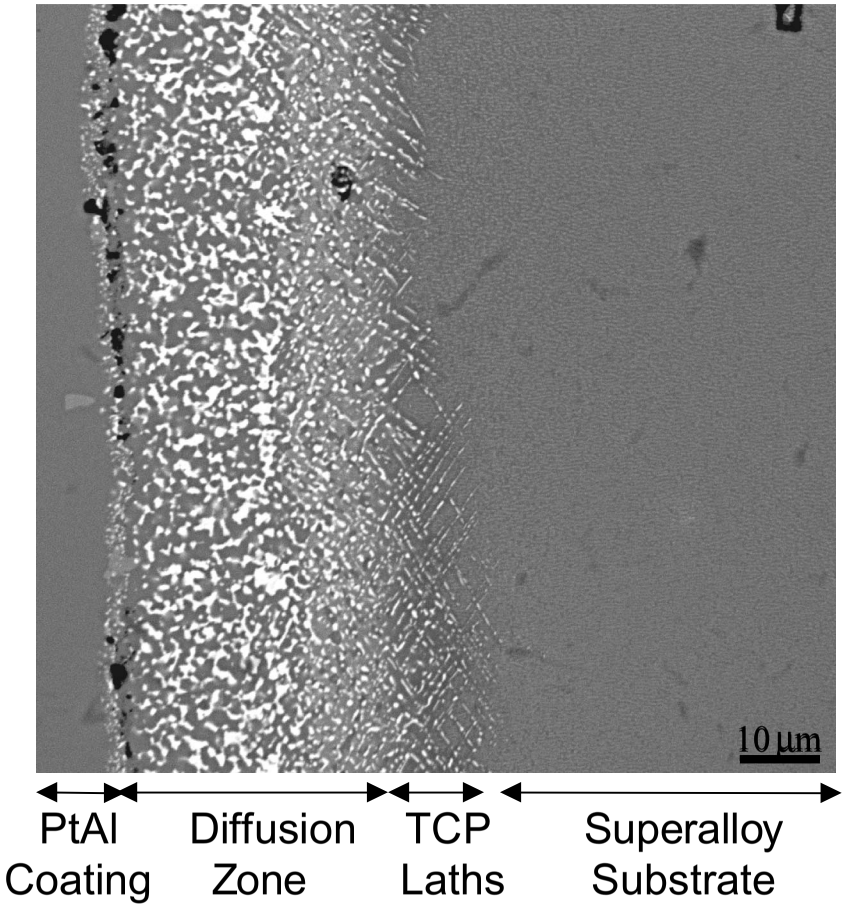

Figure 15. Microstructures in the vicinity of the diffusion zone for carburized samples showed that no fine-scale carbides were present under the diffusion zone as a result of carburization. TCP laths formed under the diffusion zone in areas with no SRZ. It is suspected that carburization was performed to insufficient depths in the substrate. EPM102A is the superalloy substrate in this photomicrograph.

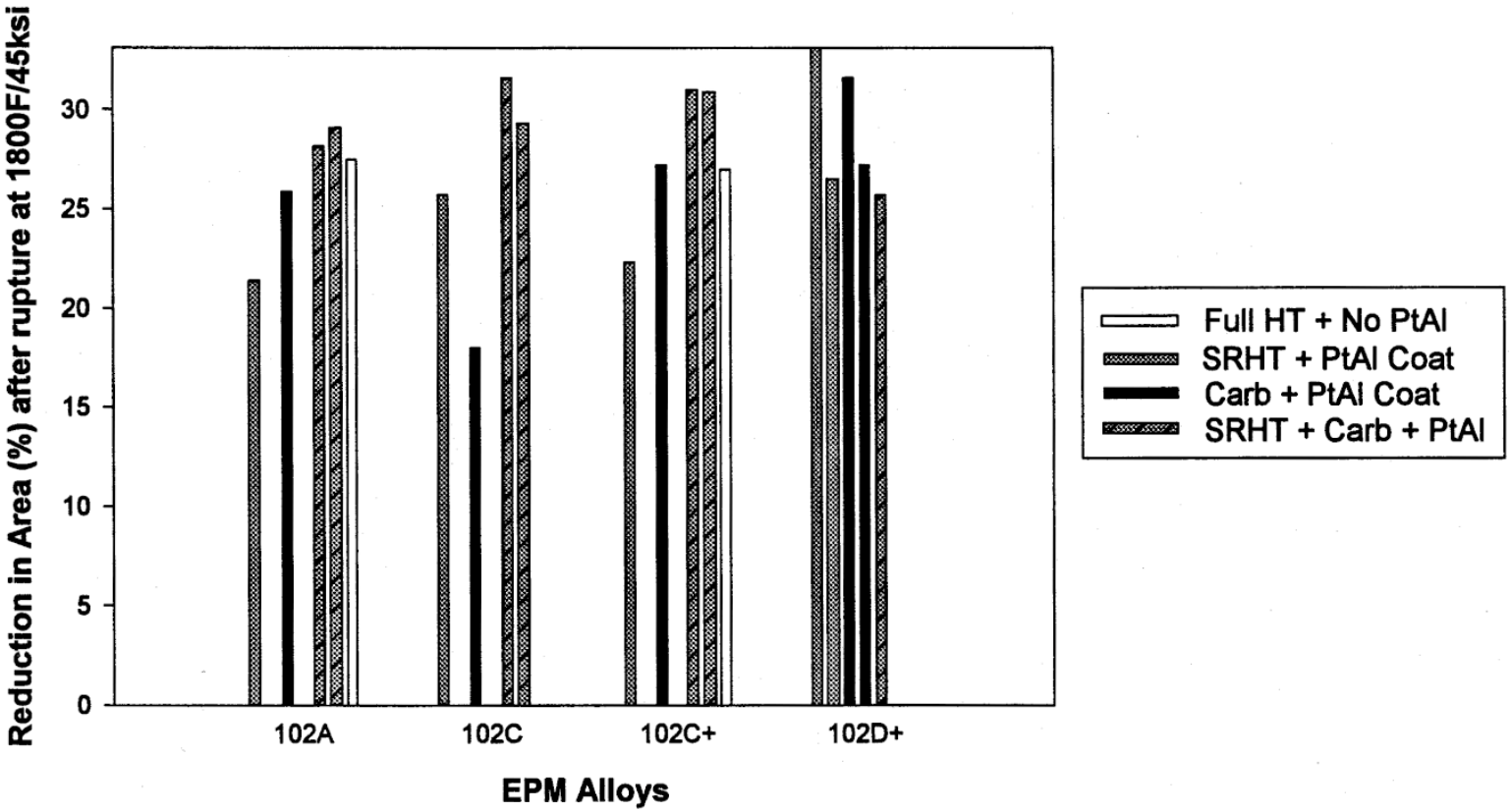

Figure 16. Reductions in area (RA) for uncoated and PtAl-coated specimens after creep-rupture testing at 1800°F and 45 ksi. The open bars respresent uncoated specimens; filled bars represent coated specimens with various SRZ-reduction treatments. All tests were conducted at NASA GRC.

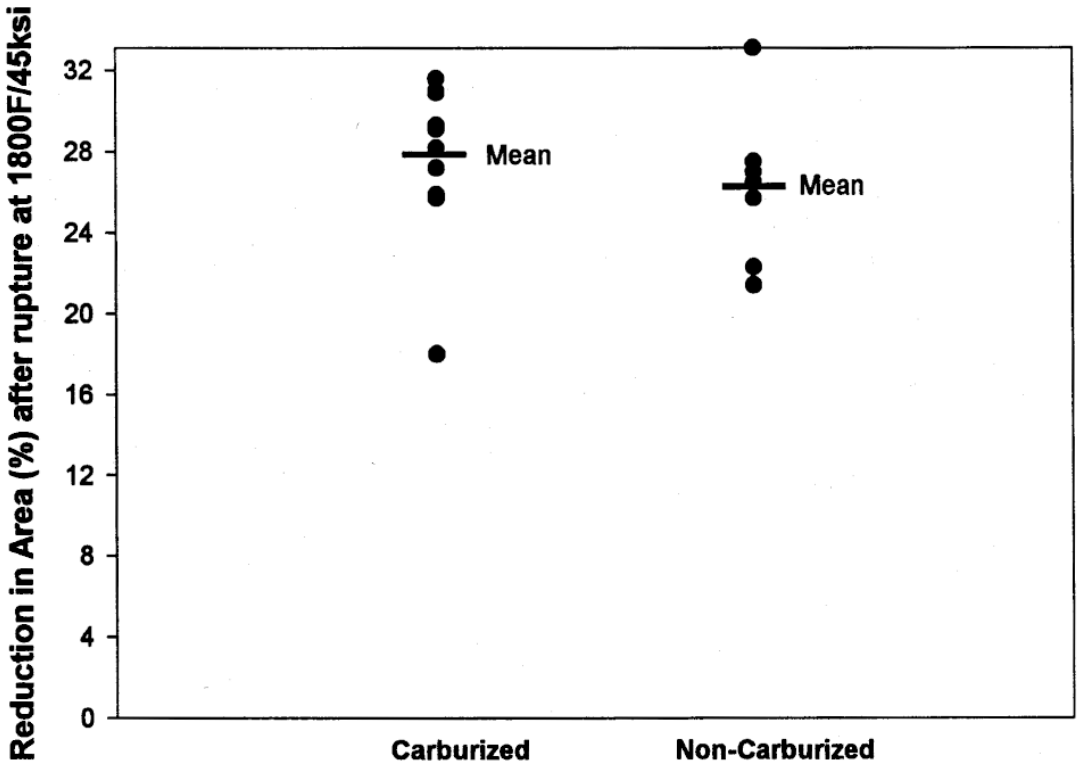

Figure 17. Reduction in area (RA) for carburized and non-carburized specimens of EPM102A, EPM102C, EPM102C+, and EPM102D+ after creep-rupture testing at 1800°F and 45 ksi. All tests were conducted at NASA GRC.

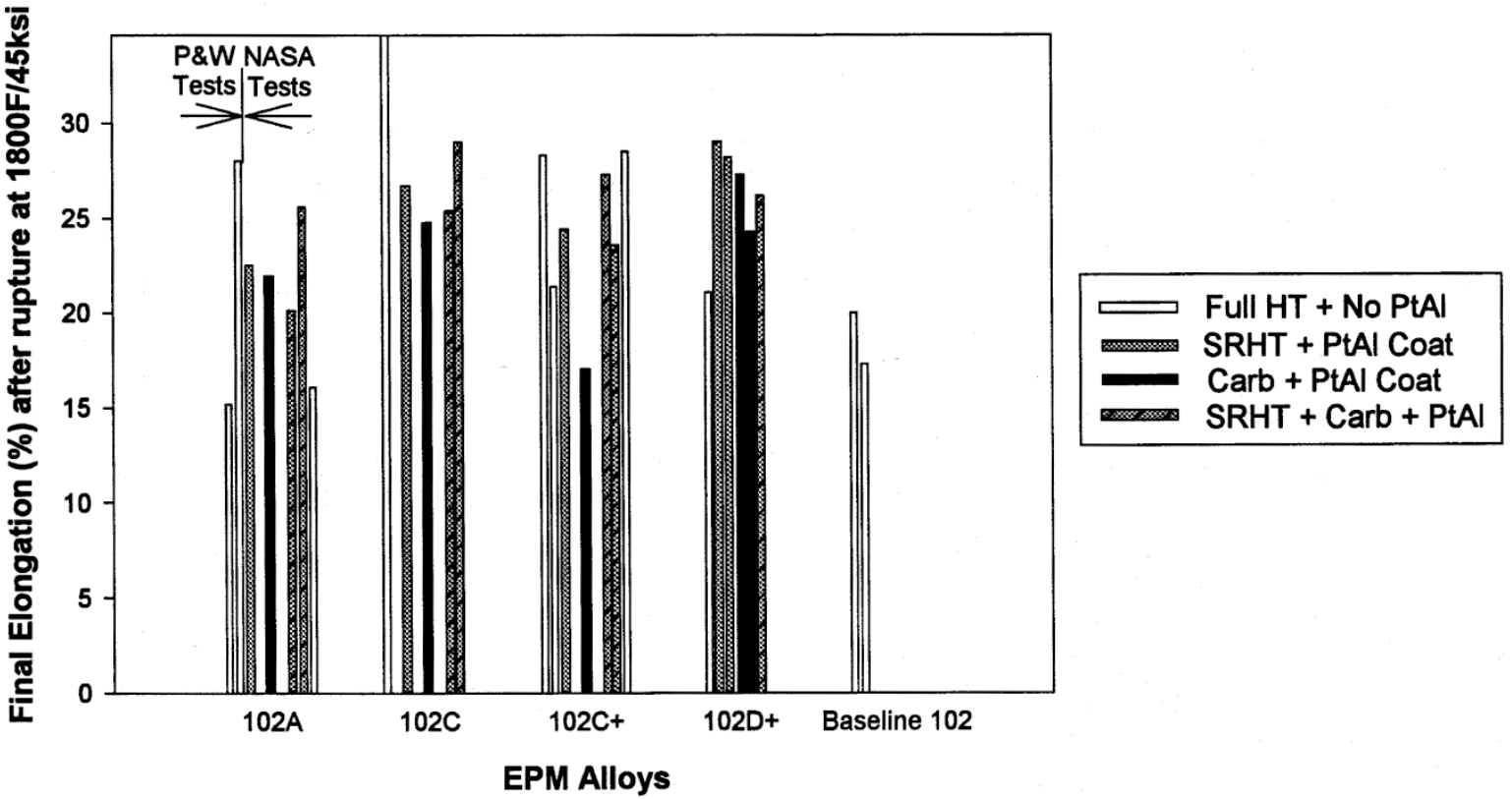

Figure 18. Elongations for uncoated and PtAl-coated specimens after creep-rupture testing at 1800°F and 45 ksi. The open bars respresent uncoated specimens; filled bars represent coated specimens with various SRZ-reduction treatments. The first two neighboring open bars for each alloy represent test results from a P&W vendor; the remaining bars for each alloy represent test results generated at NASA GRC. The two bars for the Baseline 102 alloy represent test results from a P&W vendor.

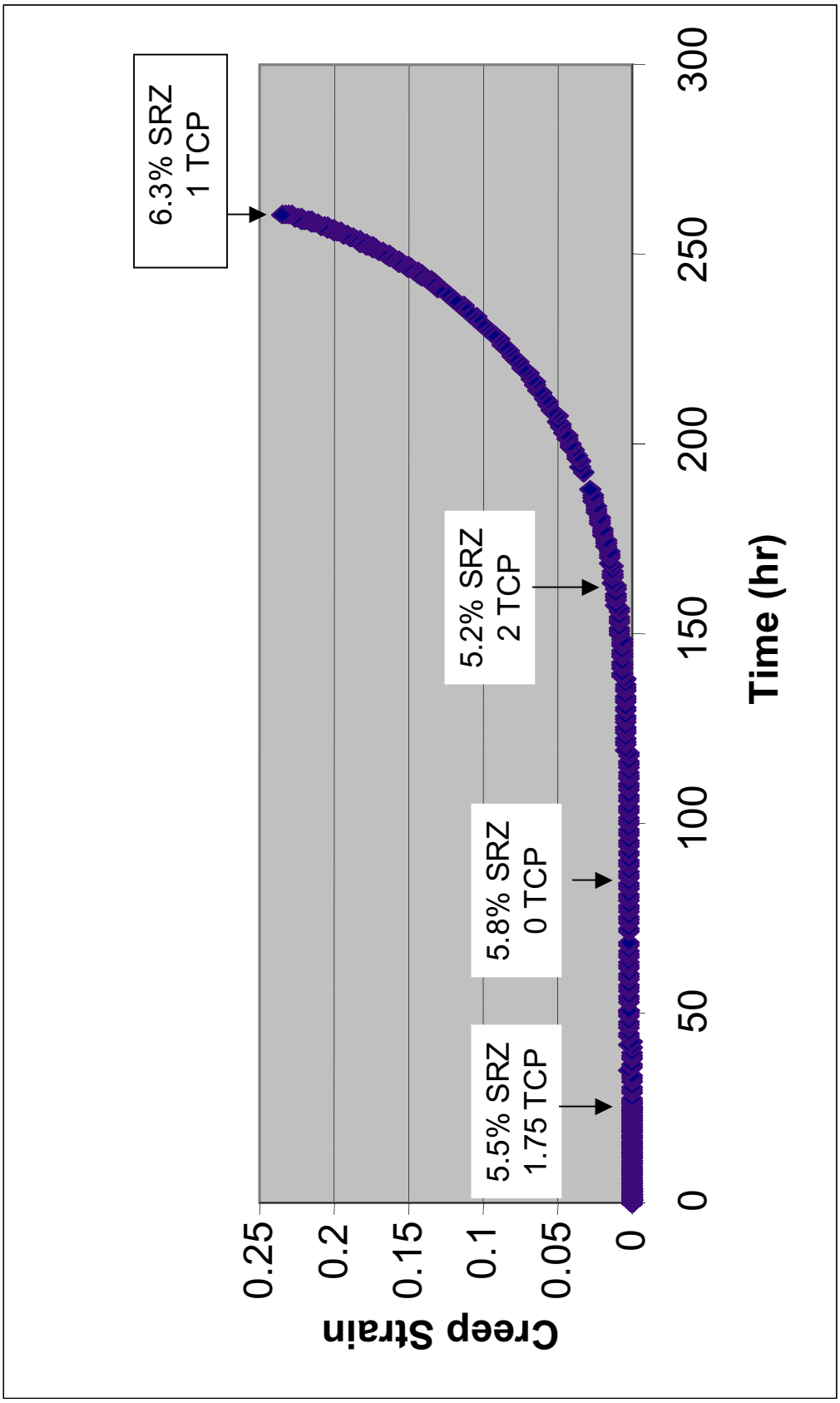

Figure 19. Creep curve of PtAl-coated EPM102D+ specimen at 1800°F and 45ksi. Specimen exhibited a creep rupture life of 261 hr. Interrupted tests were also conducted at 25, 80, and 159 hr. The amount of SRZ under the coating and the TCP level observed in each specimen have been superimposed in the figure.

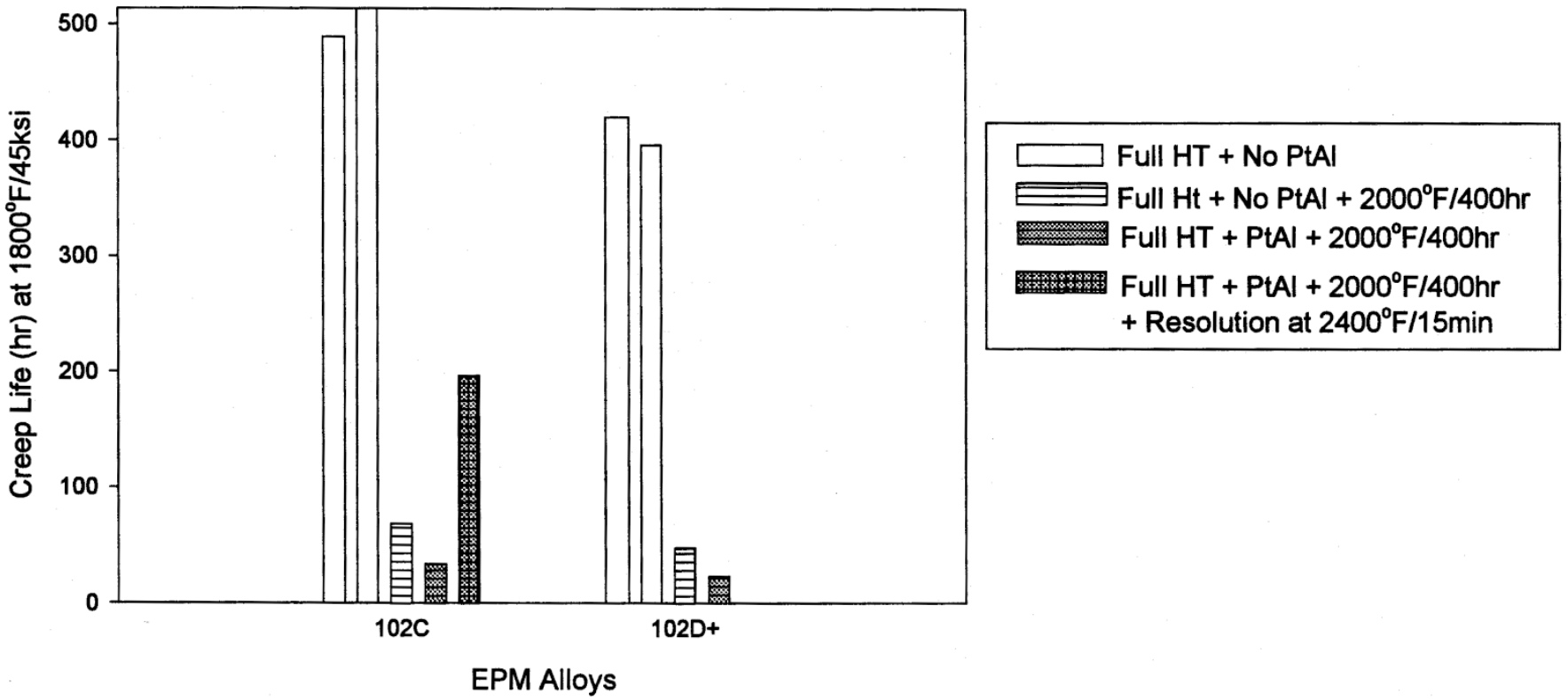

Figure 20. Creep rupture lives at 1800°F and 45ksi for uncoated and PtAl-coated EPM102C and EPM102D+. Some specimens were given an extended age at 2000°F and 400hr. One specimen was resolutioned at 2400°F for 15min in an attempt to restore part of the creep rupture life. The first two specimens of each alloy set were tested by a Pratt & Whitney vendor. The remaining specimens of each alloy set were tested at NASA GRC.

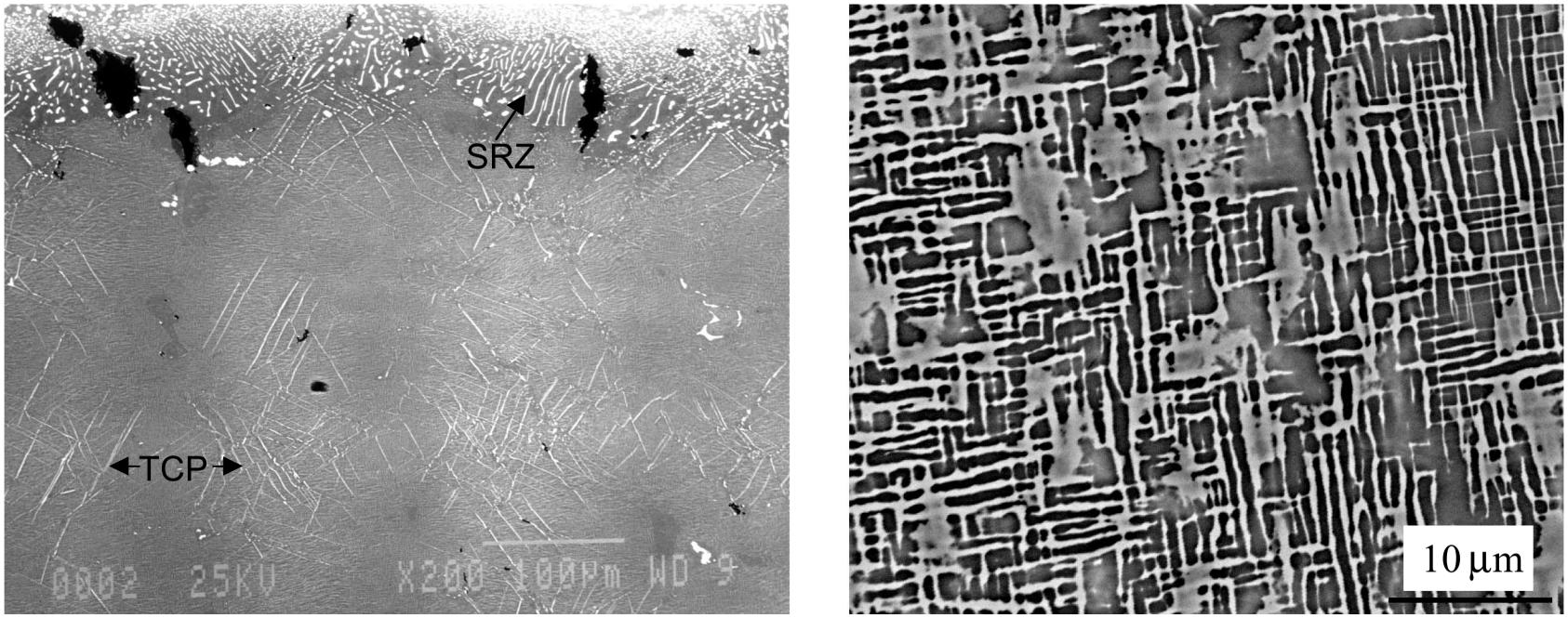

(a) (b)

Figure 21. (a) Higher levels of SRZ and TCP observed in creep rupture specimens given a pre-exposure of 2000°F for 400 hr. (b) Coarsened γ-γ' microstructure after full heat treatment, consisting of a 2050°F/4-hour stress-relief, the PtAl-coating cycle, and a 1600°F age for 12 hours, followed by aging an additional 400hr at 2000°F.

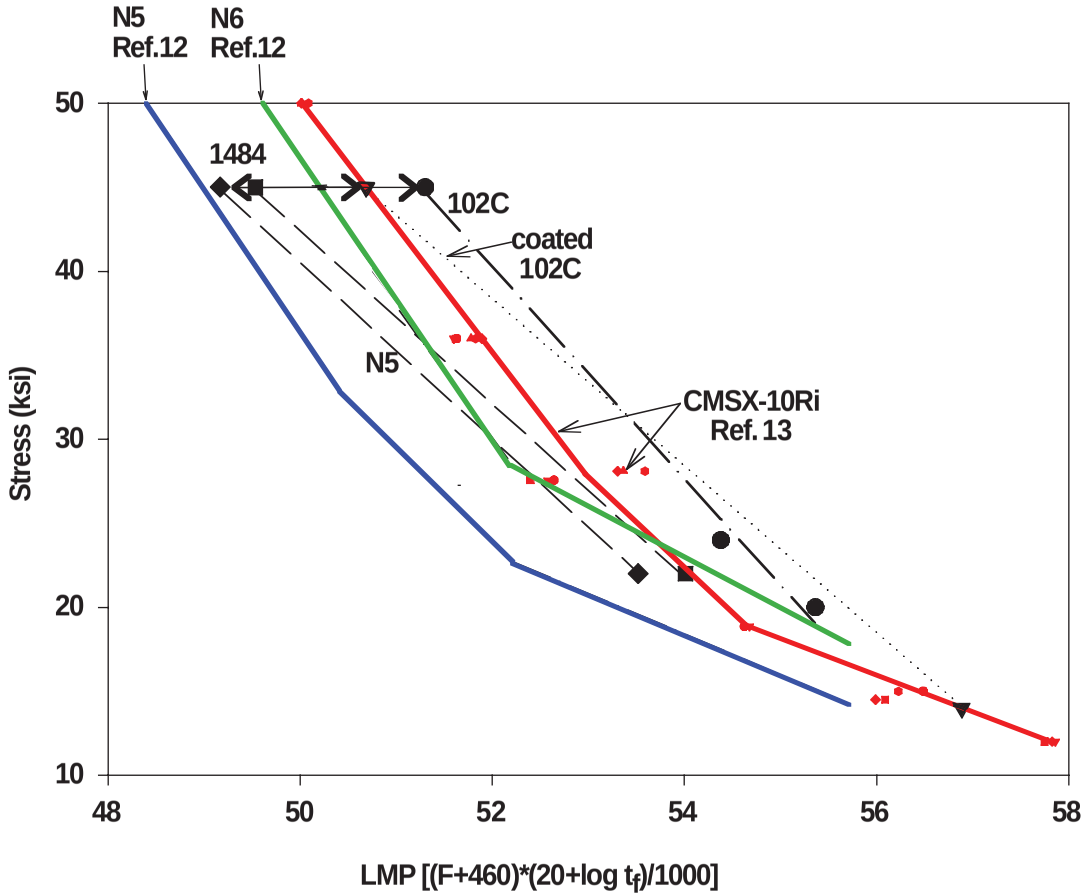

Figure 22. Larson Miller Parameter Curves for various alloys. Coated EPM102C data at 45 ksi was generated at NASA GRC. EPM 102C (uncoated) was generated at a Pratt & Whitney vendor. Rene N5 and PWA 1484 data were generated in the EPM Program (Ref. 2) and served as the programmatic baseline. These data are represented by the long dashed lines between 45 and 22 ksi. For comparison, creep rupture data obtained from the literature are shown for Rene N5 and Rene N6 (Ref. 12) and CMSX-10Ri (Ref. 13).

REPORT DOCUMENTATION PAGE	Form Approved OMB No. 0704-0188

The public reporting burden for this collection of information is estimated to average 1 hour per response, including the time for reviewing instructions, searching existing data sources, gathering and maintaining the data needed, and completing and reviewing the collection of information. Send comments regarding this burden estimate or any other aspect of this collection of information, including suggestions for reducing this burden, to Department of Defense, Washington Headquarters Services, Directorate for Information Operations and Reports (0704-0188), 1215 Jefferson Davis Highway, Suite 1204, Arlington, VA 22202-4302. Respondents should be aware that notwithstanding any other provision of law, no person shall be subject to any penalty for failing to comply with a collection of information if it does not display a currently valid OMB control number.
PLEASE DO NOT RETURN YOUR FORM TO THE ABOVE ADDRESS.

1. REPORT DATE *(DD-MM-YYYY)*	2. REPORT TYPE	3. DATES COVERED *(From - To)*
01-12-2007	Technical Memorandum	

4. TITLE AND SUBTITLE
Assessment of Creep Capability of HSR-EPM Turbine Airfoil Alloys

5a. CONTRACT NUMBER

5b. GRANT NUMBER

5c. PROGRAM ELEMENT NUMBER

6. AUTHOR(S)
MacKay, Rebecca, A.; Garg, Anita; Ritzert, Frank, J.; Locci, Ivan, E.

5d. PROJECT NUMBER

5e. TASK NUMBER

5f. WORK UNIT NUMBER
WBS 984754.02.07.03.11.03

7. PERFORMING ORGANIZATION NAME(S) AND ADDRESS(ES)
National Aeronautics and Space Administration
John H. Glenn Research Center at Lewis Field
Cleveland, Ohio 44135-3191

8. PERFORMING ORGANIZATION REPORT NUMBER
E-16143

9. SPONSORING/MONITORING AGENCY NAME(S) AND ADDRESS(ES)
National Aeronautics and Space Administration
Washington, DC 20546-0001

10. SPONSORING/MONITORS ACRONYM(S)
NASA

11. SPONSORING/MONITORING REPORT NUMBER
NASA/TM-2007-214921

12. DISTRIBUTION/AVAILABILITY STATEMENT
Unclassified-Unlimited
Subject Category: 26
Available electronically at http://gltrs.grc.nasa.gov
This publication is available from the NASA Center for AeroSpace Information, 301-621-0390

13. SUPPLEMENTARY NOTES

14. ABSTRACT
The High Speed Civil Transport (HSCT) mission of the High Speed Research-Enabling Propulsion Materials (HSR-EPM) Program represented a unique challenge for turbine airfoil materials because the highest operating temperatures occur during climb and supersonic cruise. The accumulated hot time of an HSCT engine before overhaul is many thousands of hours. This is significantly different from subsonic engines, where the maximum operating temperatures occur during takeoff and thrust reverse after landing, and the accumulated hot time before overhaul is about 300 hr. The goal of airfoil alloy development under the HSR-EPM Program was to develop an alloy with a 75 °F increase in creep rupture capability over the average Rene N5/PWA 1484 baseline. Airfoil alloy development under the HSR-EPM Program pursued a path that led to evolutionary mechanical behavior improvements, resulting from increased amounts of high density, refractory metals. The purpose of the present paper is to describe the experimental work that was performed at NASA Glenn Research Center after the HSR-EPM Program ended. Emphasis will be placed on the creep behavior of coated specimens, as well as on the development and progression of phase instabilities during creep deformation. Mitigation techniques that were used to reduce phase instabilities are also discussed. Most of the work described in this report was performed at NASA Glenn during the years 2000 and 2001.

15. SUBJECT TERMS
Single crystals; Turbine blades; High temperature; Microstructure; Creep strength; Superalloys

16. SECURITY CLASSIFICATION OF:			17. LIMITATION OF ABSTRACT	18. NUMBER OF PAGES	19a. NAME OF RESPONSIBLE PERSON
a. REPORT	b. ABSTRACT	c. THIS PAGE			STI Help Desk (email:help@sti.nasa.gov)
U	U	U	UU	45	19b. TELEPHONE NUMBER *(include area code)* 301-621-0390